Inhibitory interneurons with differential plasticities at their connections tune excitatory–inhibitory balance in the spinal nociceptive system

Lou Cathenaut, Benjamin Leonardon, Robin Kuster, Perrine Inquimbert, Rémy Schlichter, Sylvain Hugel

Title:

Inhibitory interneurons with differential plasticities at their connections tune excitatory/inhibitory balance in the spinal nociceptive system

Authors

Lou Cathenaut[1], Benjamin Leonardon[1], Kuster Robin[1], Perrine Inquimbert[1], Rémy Schlichter[1], Sylvain Hugel[1]*

[1]Centre National de la Recherche Scientifique, Université de Strasbourg, Institut des Neurosciences Cellulaires et Intégratives, 67000 Strasbourg, France.

Number of pages: 43

Number of figures: 7

Number of supplementary figures: 8

Number of supplementary tables: 7

*** Corresponding author**

Centre National de la Recherche Scientifique, Université de Strasbourg, Institut des Neurosciences Cellulaires et Intégratives, 8 allée du Général Rouvillois, F-67000 Strasbourg

hugels@inci-cnrs.unistra.fr

Phone: +33388456666

Conflict of interest statement. The authors declare no competing financial interests.

Abstract

Networks of the dorsal-horn of the spinal-cord process nociceptive information from the periphery. In these networks, the excitation/inhibition balance is critical to shape this nociceptive information and to gate it to the brain where it is interpreted as pain. Our aim was to define whether short-term plasticity of inhibitory connections could tune this inhibition/excitation balance by differentially controlling excitatory and inhibitory microcircuits. To this end, we used spinal-cord slices from adult mice expressing enhanced green fluorescent protein (eGFP) under the GAD65 promoter and recorded from both eGFP+ (putative inhibitory) and eGFP- (putative excitatory) neurons of lamina II while stimulating single presynaptic GABAergic interneurons at various frequencies. Our results indicate that GABAergic neurons of lamina II simultaneously contact eGFP- and eGFP+ neurons, but these connections display very different frequency-dependent short-term plasticities. Connections onto eGFP- interneurons displayed limited frequency-dependent changes, and strong time-dependent summation of inhibitory synaptic currents that was however subjected to a tonic activity-dependent inhibition involving A1 adenosine receptors. In contrast, GABAergic connections onto eGFP+ interneurons expressed pronounced frequency-dependent depression, thus favoring disinhibition at these synapses by a mechanism involving the activation of $GABA_B$ autoreceptors at low frequency. Interestingly, the balance favors inhibition at frequencies associated with intense pain whether it favors excitation at frequencies associated with low pain. Therefore, these target- and frequency-specific plasticities allow to tune the balance between inhibition and disinhibition while processing frequency-coded information from primary afferents. These short-term plasticities and their modulation by A1 and $GABA_B$ receptors might represent an interesting target in pain-alleviating strategies.

Introduction

Nociceptive information conveyed from the periphery by primary afferents is integrated in the dorsal-horn of the spinal-cord before being forwarded to the brain where it can lead to pain perception. Among sensory neurons, C- and Aδ-primary afferents conveying nociceptive information mostly project to networks within dorsal-horn superficial layers (laminae I-III). In lamina II (LII), primary afferents synapse with local excitatory or inhibitory interneurons [24; 30; 33; 34]. In turn, LII inhibitory interneurons contact either excitatory or inhibitory interneurons [24; 33; 34; 44; 54]. Inhibitory interneurons in these networks play a critical role in the processing of nociceptive information, and alteration of inhibition is associated with physiological/pathological pain states [23; 39; 48; 50]. LII interneurons are inhibited by both GABAergic and glycinergic connections but local inhibitory connections between LII neurons are mostly GABAergic [27; 33].

Sensory neurons projecting to these networks encode the intensity of adequate stimuli using an action-potential frequency code [1; 2; 7; 51]. In other regions of the central nervous system, the processing of such frequency-coded information is known to involve frequency-selective synapses [13; 26; 29]. These synapses display short-term plasticity (STP) processes changing dynamically their efficacy over time as a function of the delay between presynaptic action-potentials [6; 37]. Therefore, networks in the spinal nociceptive system are also expected to display short-term plasticity in order to process frequency-coded sensory information. Surprisingly, this question has been little addressed experimentally, and has mostly used simple paired-pulse stimulation protocols [8; 20; 24; 43; 53] and very rarely protocols using trains of stimulations [9; 20; 27; 53].

Data on the impacts of stimulation trains in information processing in the dorsal-horn are also pending to fully understand the mechanisms engaged by the rapidly-expanding stimulation approaches used in pain alleviation such as spinal-cord stimulation [17; 22]. Together with other targets, this approach has indeed been suggested to activate inhibitory LII interneurons [11].

The objective of the present study was to examine short-term plasticities of GABAergic connections onto LII neurons, and to determine whether such plasticities were different when the synapses involved an excitatory or an inhibitory postsynaptic (target) neuron. To this end, we prepared acute slices from mice expressing enhanced green fluorescent protein (eGFP) under the control of the GAD65 promoter [10]. We recorded from either eGFP-expressing (eGFP+) or eGFP negative (eGFP-) neurons, and also performed simultaneous recordings of eGFP+ and eGFP- neurons while stimulating single presynaptic GABAergic neurons.

Our results indicate that GABAergic connections onto eGFP+ neurons of LII display different short-term plasticities than those onto eGFP- neurons, favoring inhibition at frequencies occurring during intense nociceptive stimulation and favoring excitation at frequencies occurring during nociceptive stimulation of low intensity.

Methods

Animals

For all experiments, we used male heterozygous C57BL/6 BAC transgenic mice eGFP under the control of the GAD65 promoter obtained from Ferenc Erdelyi and Gabor Szabo (Institute of Experimental Medicine, Budapest) [10]. In these mice, ~80% of LII eGFP+ neurons are GABA-immunopositive and ~60% of GABA-immunopositive neurons are eGFP+ [10]. These mice were interbred at the local animal facility, The Chronobiotron (agreement number: A67-2018-38). The

animals were housed at room temperature (22-25°C) with a 12hr light/dark cycle with free access to food and water. All procedures used were in accordance with laws for laboratory animal welfare and approved by the local ethical committee of the University of Strasbourg (CREMEAS; agreement number: APAFIS#8138-2016121008385362 v3).

Slicing procedure

Adult transgenic mice (5-9 weeks) were anaesthetized with urethane (1.9 $g.kg^{-1}$). Under deep anesthesia, intracardiac perfusion was performed with oxygenated ice-cold (~4°C) sucrose artificial cerebrospinal fluid (sACSF) bubbled with carbogen (95% O_2, 5% CO_2) containing (in mM): 248 sucrose, 26 $NaHCO_3$, 11 glucose, 2 KCl, 2 $CaCl_2$, 1.3 $MgSO_4$, 1.25 KH_2PO_4, 2.5 kynurenic acid. The lumbar part (L3-L5) of the spinal cord was removed by laminectomy and 400 µM thick transverse slices were cut with a vibrating microtome (Leica, VT1200S). Slices were kept until recording at room temperature (~25°C) in oxygenated ACSF containing in mM: 126 NaCl, 2.5 KCl, 2 $CaCl_2$, 2 $MgCl_2$, 26 $NaHCO_3$, 1.25 NaH_2PO_4, 10 glucose.

Patch-clamp recordings

After recovery (~1 h), slices were transferred to the recording chamber, maintained at 32 ± 1°C and continuously perfused by oxygenated ACSF at 3-4 ml/min. In order to isolate GABAergics IPSCs, glycinergic and glutamatergic ionotropic transmissions were blocked by adding in ACSF 1 µM strychnine and 10 µM 6-cyano-7nitroquinoxaline-2,3-dione (CNQX) respectively. Whole-cell patch recordings were made from inhibitory (eGFP+) and putative excitatory (eGFP-) LII neurons. Recording and extracellular stimulation electrodes (4-7 MΩ) were pulled from borosilicate glass capillaries (1.2 mm inner diameter, 1.69 mm outer diameter, Warner Instruments, Harvard

Apparatus) using a P1000 electrode puller (Sutter Instruments). Recording electrodes were filled with, in mM: 140 KCl, 2 MgCl, 10 HEPES, 2 MgATP; pH 7.3. In experiments using increased stimulation amplitudes, 1 mM QX314 was added to this intrapipette solution to prevent spiking of the recorded neuron. Junction potentials were not corrected. Whole-cell patch clamp recordings (in current-clamp and voltage-clamp recording modes) were made using a Multiclamp 700A amplifier (Molecular Devices). Signals were low-pass filtered at 5 kHz, sampled at 20 kHz, digitized using a BNC-2110 data acquisition card (National Instruments) and acquired with the Strathclyde electrophysiology software (WinWCP, John Dempster, University of Strathclyde, Glasgow, UK).

Experimental design

Our recordings started in the current-clamp mode. Holding current was adjusted in order to keep the recorded neuron at a membrane potential of -60 mV. In this mode, firing patterns were determined in response to 1 s-long depolarizing current injections through the recording electrode (20-80 pA in 20 pA steps). For some experiments in the current-clamp mode, we simulated excitatory synaptic potentials (EPSPs) by injecting EPSCs current traces. These EPSCs current traces were constructed by averaging excitatory postsynaptic currents evoked by local electrical extracellular stimulation (EPSCs) recorded in LII neurons (same protocol as for eIPSCs described below) with 10 µM bicuculline and 1 µM strychnine. In these conditions, average eEPSCs was of 88.9 ± 10.6 pA with a rise time of 2.1 ± 0.3 ms and a decay time constant of 5.7 ± 0.9 ms (n = 4 neurons). To simulate the convergence of excitatory inputs as suggested by Grudt & Perl (2002) who recorded C-fibrers mediated EPSCs in islet cells of above 400 pA, we injected the current corresponding to 4 times the average eEPSC we measured.

After this initial phase, neurons were recorded in the voltage-clamp mode at a holding potential of -60 mV. Monosynaptic IPSCs were evoked by local extracellular electrical stimulation. This stimulation was performed by applying current steps (0.25 ms; 0.10-0.40 mA; average 0.21 ± 0.01 mA) via a patch-pipette filled with ACSF. This stimulation electrode was placed at a distance of 20-150 µm from the cell body of the recorded neuron. For each recorded neuron, the lowest amplitude of stimulation evoking inhibitory postsynaptic currents was determined. This amplitude was increased by 0.05 mA to evoke inhibitory postsynaptic currents (eIPSCs) for each stimulation applied. Synaptic contacts were identified as monosynaptic unitary connections when the following criteria were satisfied: (1) all-or-none appearance of eIPSCs, (2) absence of increase in eIPSC amplitude when minimal stimulation amplitude was increased by 0.05 mA, (3) disappearance of eIPSCs when stimulation polarity was inverted, and (4) constant latency of the eIPSCs.

The same criteria were applied for simultaneous recordings of pairs of eGFP- and eGFP+ neurons connected by the same presynaptic neuron.

For all neurons, paired-pulse stimulations were applied with an inter-stimulation interval (ISI) of 200 ms repeated every 10 s. In a subset of neurons, paired-pulse stimulations with multiple ISIs were applied (ISIs of 20, 50, 75, 100, 200, 300 ms) and pairs of stimulation were separated by 10 s. Trains of 11 stimulations repeated 10 times were used in most experiments. Unless otherwise stated, trains applied at 5 Hz were repeated every 20 s whereas trains applied at 50 Hz were applied every 60 s.

Data quantification and analysis

158 Action-potential firing patterns were analyzed offline using Clampfit 10 (Molecular Devices, USA).
159 Neurons firing multiple spikes during the whole duration of the depolarizing current step and
160 displaying a constant interval between each spike were classified as Tonic-firing type (tonic) (Fig.
161 1A); neurons with a burst of spikes at the beginning of depolarizing current step and showing a
162 decrease in inter-spike interval duration during the step as well as a progressive reduction of
163 spike amplitudes were classified as Initial bursting type (IB) (Fig. 1A); neurons fulfilling neither of
164 these criteria were classified as “Other type” of firing pattern.
165 eIPSCs were also analyzed offline using Clampfit 10. Synaptic inhibitory transmission was
166 quantified by measuring the amplitude of individual eIPSCs. To take into account baseline
167 changes due to eIPSCs summation, the amplitude immediately before stimulation was subtracted
168 from the peak amplitude of each eIPSC. Unless otherwise stated, stimulation protocols were
169 applied ten times in each neuron and the within-cell average across trials was calculated by
170 averaging eIPSCs amplitudes from these ten repetitions. When protocols consisted of trains of
171 stimulations, amplitudes of eIPSCs of the same rank in the train were averaged. These within-cell
172 average across ten trials were used for statistical analysis (Fig. S1).
173 Averaging amplitudes of raw eIPSCs gives greater weight to connections in which eIPSCs display
174 larger amplitudes. Therefore, in addition to analyzing raw eIPSCs amplitudes, we calculated
175 normalized eIPSCs amplitudes. These were calculated by normalizing for each neuron the
176 averaged eIPSCs amplitudes to the averaged amplitude of the first eIPSCs in the train. This
177 allowed to analyze relative changes in amplitude during trains regardless of the initial raw
178 amplitude values of eIPSCs.
179 Both raw and normalized eIPSCs amplitudes were used for statistical analysis.

For paired-pulse stimulation experiments, the paired-pulse ratio (PPR) was calculated as the amplitude of the second eIPSC divided by the amplitude of the first eIPSC.

The weighted decay time constant (τ_w) was calculated as described in Labrakakis et al. [28] from biexponential fits using equation 1.

Equation 1. $\tau_w = (\tau_f \cdot A_f + \tau_s \cdot A_s)/(A_f + A_s)$

where τ_f and τ_s are the fast and slow decay time constants, respectively and A_f and A_s the corresponding amplitudes used as weighting factors.

For experiments with $GABA_B$ and A1 antagonists, trains of stimulations were repeated before, during and after perfusion of the antagonists. Ten trains were applied in control conditions and the antagonist was subsequently applied for 10 minutes. The effect of antagonists was measured after at least 3 minutes of perfusion. For each neuron, amplitudes of eIPSCs of the same rank in the two conditions (i.e. control vs. antagonist) were averaged. Results are expressed as mean ± SEM.

For some experiments, we recorded miniature IPSCs. These synaptic events were detected using WinEDR (V3.8.6, Strathclyde Electrophysiology Software, John Dempster, University of Strathclyde, Glasgow, UK) with an amplitude threshold detection algorithm and were visually inspected for validity. Peak amplitude of miniature IPSCs was determined using WinWCP (version 5.4.5). Events were detected during at least 200 s.

Statistics

Statistical analysis were performed using averaged eIPSCs amplitudes (i.e. within-cell average across trials) of each neurons (Fig. S1). These were calculated for each neuron by averaging

amplitudes of eIPSCs of the same rank (2 ranks for paired-pulse experiments, 11 ranks for trains of stimulations). The number of neurons is given as the n-value in the result section.

Student's *t*-test was used to compare amplitudes of isolated eIPSCs, decay time constants and mIPSCs after having tested for data normality (Kolmogorov-Smirnov test, $p > 0.05$).

For paired-pulse protocols, the proportions of neurons displaying a facilitation (PPR>1.1), a depression (PPR<0.9) or no change in PPR (0.9-1.1) were analyzed with a log-linear analysis performed on the 3-way contingency table of the proportion of facilitation, ISI and eGFP+/eGFP- condition using Statistica 13 (StatSoft, USA). The χ^2 values and p-values given in the text correspond to those of marginal associations between the two parameters examined. To compare amplitudes of the two first eIPSCs during stimulation trains protocols, Wilcoxon Signed Rank Test for Paired Data was used since data were not always normally distributed.

Non-linear regression analysis [38] was used to analyze PPR values as a function of ISIs and changes in eIPSCs amplitudes during stimulation train protocols. Individual data of all neurons were always used for curve fitting and average values were used for illustration (Fig. S1).

PPR values as a function of ISIs for eGFP+ and eGFP- neurons were fitted with the equation 2.

Equation 2. Y=A1+((A1-A2)*EXP(-X/A3))

where A1 corresponded to Y value for ISI=0; A2 corresponded to the asymptotic value of the fit; and A3 corresponded to the exponential decay constant of PPR value as a function of ISI. Parameters A1, A2 and A3 were determined by nonlinear curve fitting using KyPlot 6.0 (KyensLab, Tokyo, Japan). A global fit on the same data was also performed using the same equation. This global fit was compared to the sum of fits from separated data obtained from eGFP+ and from eGFP- neurons.

Non-linear curve fitting was used to analyze and compare changes in eIPSCs amplitudes during stimulation train protocols. This analysis was performed using averaged eIPSCs amplitudes of each neurons.

Amplitudes of eIPSCs as a function of their respective rank in the train were fitted using the equation 3.

Equation 3. $Y=A1+A2*(1-EXP(-X/A3))$

where A1 corresponded to Y value of the 1st eIPSCs of the train, A2 corresponded to the change in amplitude for the curve asymptote, A3 corresponded to the constant of the exponential function.

A1 and A2 are in pA for fits of raw eIPSCs amplitudes and are dimensionless for fits of normalized eIPSCs amplitudes. A3 unit is the rank of stimulation in the train.

To define whether STP was expressed during trains of stimulations, i.e. whether significant changes in amplitude occurred during the train, fits with Equation 3 were compared with linear fits with slope values forced to 0. When fits with Equation 3 provided statistically significant improvements with respect to the linear fit with slope value forced to 0, the connections were considered as displaying a significant STP during the corresponding protocol [38].

To compare two different conditions (e.g. eGFP- vs. eGFP+ or presence/absence of antagonists) data from each conditions were fitted with Equation 3, either individually (sum of two functions) or pooled (one single function). When the sum of two individual fits provided statistically significant improvements with respect to the fit of pooled data, the two conditions were considered as having distinct effects [38]. Fits of pooled data are illustrated (in black) when the two conditions were not different whereas individual fits are illustrated (in color) when the two

conditions were significantly different. For illustration purpose, these fits are illustrated together with the averages of "cross-trial averages".

In the result section, p-value of model comparisons are given as well as the corresponding number of neurons (n). The significance level used for all analysis was set at 0.05. The goodness-of-fit was also compared by calculating for both conditions Bayesian Information Criterion (BIC), Akaike Information Criterion (AIC), and the corresponding sample-size bias-corrected values (AICc) [47]. A model was considered as better if model comparison p-value was < 0.05 and if the model provided a reduction in AICc. The only case where the p-value and AICc are in conflict ($p < 0.05$ and increase in AICc for the effect of DPCPX on eGFP+ neurons) is mentioned in the result section. Details of all models (A1, A2, A3, degree of freedom, Residual sum of squares, AIC, AICc, BIC) as well as details of model comparison (F, P, differences in AIC, AICc and BIC) are given in Supplementary tables 1-7.

Drug application / Pharmacology

All pharmacological agents were bath-applied. 1 µM strychnine and 10 µM CNQX were present in all our electrophysiologial experiments to isolate GABAergic eIPSCs. CGP55845 ((2S)-3-[[(1S)-1-(3,4-Dichlorophenyl)ethy]amino-2hydroxypropyl](phenylmethyl)phosphinic acid hydrochloride; 10 µM, Tocris) and DPCPX (8-Cyclopentyl-1,3-dipropylxanthine solid; 10 µM, Sigma) were used to block $GABA_B$ receptors and Adenosine A1 receptors, respectively. In a subset of experiments, eEPSCs were recorded in presence of strychnine (1 µM) and bicuculline (10 µM, sigma). Miniature IPSCs were recorded in the presence of tetrodotoxin (TTX) (0.5µM, Latoxan). CNQX and CGP55845 were dissolved in DMSO, DPCPX was dissolved in ethanol and strychnine in water; all were prepared as x10000 concentrated stock solutions. For experiments with these

antagonists, analysis of changes in normalized eIPSCs amplitudes allowed to detect modulations engaged during the train (phasic modulation). All substances were diluted to their final concentration in ACSF at the beginning of each experiment.

Results

Firing properties of eGFP+ and eGFP- neurons

LII neurons responded to sustained depolarizing current injections with various patterns of action-potential firing [19; 24; 34]. Two main firing patterns dominated (Fig. 1AB, S2): To type (40 %, 51/128) and IB type (34 %, 43/128). Other firing patterns were less frequently observed (altogether 27 %, 34/128). Most of eGFP- neurons displayed an IB firing pattern (46 %, 28/61), and a lower proportion of Tonic (36 %, 11/61) and other firing patterns (18 %, 22/61). Most of eGFP+ neurons displayed a Tonic firing pattern (60 %, 40/67), and a lower proportion of IB (22%, 15/67) and other firing patterns (18 %, 12/67). The proportions of IB, Tonic and other firing patterns in eFGP- and eGFP+ neurons were significantly different (Fisher's exact test, $P = 6.3 \cdot 10^{-6}$, Fig. 1B). The average firing frequency of both eGFP- IB neurons and eGFP+ Tonic neurons was above 50 Hz during the first 200 ms of 80 pA current steps (95.1 ± 11.9 Hz and 52.4 ± 5.7 Hz, respectively, Fig. 1C). When EPSPs were simulated by injection of EPSCs at 50 Hz during 200 ms, the proportion of EPSPs triggering an action-potential was of 79.1 ± 13.0 % in eGFP- neurons (n = 7) and of 100.0 ± 13.0 % in eGFP+ neurons which occasionally discharge more than one action potential per simulated EPSP (n = 4; Fig. 1DE). These data indicate that neurons of LII are able to discharge action-potentials at several tens of hertz, at least during few hundreds of milliseconds.

GABAergic synaptic transmission in LII

Average amplitude of pharmacologically-isolated eIPSCs (Fig. 2A) was not significantly different when recorded in eGFP- neurons (-60.5 ± 5.1 pA; n = 54) or in eGFP+ neurons (-55.6 ± 4.4 pA; n = 49); unpaired Student's *t*-test, t = -0.709, df = 101, P = 0.48. eIPSCs were evoked at similar stimulation amplitude intensity in eGFP- neurons (0.21 ± 0.01 mA; n = 53) or in eGFP+ (0.21 ± 0.01 mA; n = 45), unpaired Student's *t*-test, t = 0.176, df = 96, P = 0.86.

The weighted decay time constant (τ_w) measured for isolated eIPSCs (Fig. 2B) was not significantly different when recorded in eGFP- neurons (32.8 ± 2.8 ms; n = 29) or in eGFP+ neurons (31.1 ± 4.5 ms, n = 18); unpaired Student's *t*-test, t = -0.340, df = 45, P = 0.736.

In the same preparation, amplitude of miniature IPSCs (mIPSCs, Fig. 2C) was not significantly different when recorded in eGFP- neurons (-16.7 ± 0.9 pA; n = 9) or in eGFP+ neurons (-17.8 ± 1.2 pA; n = 22) unpaired Student's *t*-test, t = 0.526, df = 29, P = 0.603. Therefore, eIPSCs amplitude represented on average 3 times the amplitude of mIPSCs.

Postsynaptic target-specific paired-pulse plasticity at GABAergic connections in LII

Short-term synaptic plasticity was first examined using paired-pulse stimulation protocols with various ISIs.

Inhibitory connections onto eGFP+ or eGFP- neurons can either display paired-pulse facilitation (PPR > 1.1), paired-pulse depression (PPR < 0.9) or no change in paired-pulse ratio (PPR: 0.9-1.1). Proportions of neurons in each category were significantly different in eGFP- and eGFP+ neurons (Fig. 2D; χ^2 = 11.97; P = 0.003), with a larger proportion of paired-pulse facilitation in eGFP- neurons.

Values of PPR at various ISIs were significantly different in eGFP+ and eGFP- neurons (non-linear curve fitting, $P = 7.2 \cdot 10^{-3}$, Table S1, Fig. 2E). In eGFP+ neurons, average PPR values were close to 1 at all tested ISIs whereas in eGFP- neurons, average PPR values were above 1.1 for ISIs below 100 ms and progressively decreased at longer ISIs.

These data indicate that GABAergic connections onto eGFP- neurons preferentially displayed facilitation at short ISIs, and that GABAergic connections onto eGFP+ neurons preferentially displayed depression at long ISIs. Although PPR revealed differences between connections onto eGFP+ and eGFP- neurons, incoming information from the periphery is usually under the form of trains of action-potentials rather than isolated pairs of impulses. In the following experiments we therefore examined the effect of trains of stimulations.

Short-term plasticity during 5 Hz activation of GABAergic connections in LII.

We examined the short-term synaptic plasticity expressed by GABAergic connections onto LII neurons during their repeated activation at low frequency. We applied trains of 11 stimulations at 5 Hz (Fig. 3A). These trains were repeated 10 times at an interval of 20 s. For these experiments, 54 eGFP- and 49 eGFP+ neurons were recorded (averages from individual neurons, Fig. S4A-D, Table S2).

Evolution of eIPSCs amplitudes during 5 Hz trains remained similar in the first five and the last five trains for both eGFP- and eGFP+ neurons, indicating that no train-to-train plasticity was engaged under these experimental conditions (P = 0.889, eGFP-; P = 0.312, eGFP+, Table S2, Fig. 3). Moreover, eIPSC2/eIPSC1 remained unchanged in the first five and the last five trains for connections on both eGFP- and eGFP+ neurons ($P_{eGFP-} = 0.678$, $P_{eGFP+} = 0.223$, Wilcoxon Signed

336 Rank Test for Paired Data, Fig. S6). Therefore, for each neuron, amplitudes of eIPSCs of the same
337 rank in all 10 trains were averaged.
338 Average amplitude of the first eIPSCs of 5 Hz trains was not significantly different when recorded
339 in eGFP- or eGFP+ neurons (P = 0.349). However, evolution of normalized eIPSCs amplitudes
340 during 5 Hz trains was significantly different in eGFP- or eGFP+ neurons ($P = 1.94 \cdot 10^{-14}$, Table S2,
341 Fig. 3B). Such significant difference between eGFP- and eGFP+ neurons was also observed in
342 experiments where stimulation amplitudes were increased from 0.20 mA to 0.45 mA (11 eGFP-
343 neurons and 11 eGFP+ neurons, $P_{normalized} = 8.70 \cdot 10^{-15}$, Table S3, Fig. S5) indicating that changes
344 in stimulation efficacy during trains of stimulations were unlikely to influence our results.
345 In eGFP- neurons, amplitudes of normalized eIPSCs did not significantly change (Fig. 3B, S3A)
346 indicating that no plasticity was expressed during the train ($P_{normalized} = 0.451$, Table S2).
347 Contrasting with these data, the amplitude of normalized eIPSCs recorded from in eGFP+ neurons
348 significantly decreased during the train ($P_{normalized} = 2.04 \cdot 10^{-6}$, Fig. 3B) decreasing by 20% at the
349 asymptote (see parameters of the curve fitting Table S2). Similar data were obtained for raw
350 eIPSCs amplitudes (Fig. S3A, Table S2).
351 These data indicated that on average, GABAergic connections onto eGFP- neurons displayed no
352 plasticity during 5 Hz trains, whereas connections onto eGFP+ displayed strong depression.
353
354 **Short-term plasticity during 50 Hz activation of GABAergic connections in LII.**
355 We examined the short-term synaptic plasticity expressed by GABAergic connections onto LII
356 neurons during their repetitive activation at high frequency (n = 27 eGFP- neurons and n = 19
357 eGFP+ neurons). We applied trains of 11 stimulations at 50 Hz (Fig. 4A). These trains were
358 repeated 10 times (averages from individual neurons Fig. S1E-H). In a first set of experiments,

trains were repeated with long inter-train intervals of 60 s in order to limit the development of train-to-train plasticities. In these conditions, evolution of eIPSCs amplitudes during 50 Hz trains remained similar in the first five and the last five trains for both eGFP- and eGFP+ neurons (P_{eGFP-} = 0.278; P_{eGFP+} = 0.391, Fig. 4). This indicates, that no train-to-train plasticity was engaged under these experimental conditions allowing to average the traces of the 10 trains for each neurons.

Nevertheless, whereas the plasticity remained similar in the first five and the last five trains, eIPSC2/eIPSC1 significantly decreased for connections onto eGFP- neurons but not onto eGFP+ neurons (P_{eGFP-} = 0.048, P_{eGFP+} = 0.098, Wilcoxon Signed Rank Test for Paired Data, Fig. S6) suggesting that the facilitation observed in eGFP- neurons during paired-pulse stimulation at short intervals (Fig. 2E) is replaced by other types of plasticities during repeated trains of stimulation at 50 Hz.

Evolution of eIPSCs amplitudes during 50 Hz trains was significantly different in eGFP- or eGFP+ neurons for both normalized amplitudes ($P = 1.88 \cdot 10^{-9}$, Table S4, Fig. 4B) and raw amplitudes ($P = 3.73 \cdot 10^{-8}$, Table S4, Fig. S3C). In eGFP- neurons, amplitudes of normalized eIPSCs did not significantly change indicating that no plasticity was expressed during the train ($P_{normalized}$= 0.647, Table S1.4). By contrast, the amplitude of normalized eIPSCs recorded in eGFP+ neurons significantly decreased during the train ($P_{normalized} = 9.03 \cdot 10^{-6}$, Table S4, Fig. 4B), decreasing by 28 % at the asymptote (see parameters of the curve fitting, Table S4). Similar data were obtained for raw eIPSCs amplitudes (Fig. S3C, Table S4).

These data indicated that on average, GABAergic connections onto eGFP- neurons displayed no plasticity during 50 Hz trains whereas connections onto eGFP+ strongly depressed.

Comparison of plasticities at 5 Hz and 50 Hz

382 The evolution of normalized eIPSCs amplitudes during 5 Hz and 50 Hz trains was significantly
383 different for both eGFP- neurons ($P = 5.23 \cdot 10^{-3}$, Table S5, Fig. 3B, 4B) and eGFP+ neurons ($P = 2.76 \cdot 10^{-10}$, Table S5, Fig. 3B, 4B) indicating that the characteristics of the effects depended on the
385 frequency (see parameters of the curve fitting, Table S5). In eGFP+ neurons, the decrease of
386 normalized eIPSCs during 5 Hz and 50 Hz differed in both the magnitude and the kinetic of the
387 depression. The decrease of normalized amplitudes at the asymptote was of 20 % with 5 Hz
388 protocols whereas it was of 28 % with 50 Hz protocols. In these neurons, 90 % of asymptotic
389 values were reached at the 11^{th} stimulation with 5 Hz protocols and before the 5^{th} stimulation
390 with 50 Hz protocols.
391 These data indicate that plasticities expressed by GABAergic connections depended on both the
392 neurochemical identity of the postsynaptic target neuron and the frequency of electrical activity
393 of the presynaptic GABAergic neuron.
394
395 **Summation of eIPSCs during trains at 50 Hz**
396 During 50 Hz trains, the eIPSCs had not fully returned to baseline at the onset of the following
397 stimulation, a situation that resulted in their summation. We therefore reanalyzed our data
398 measuring summed eIPSCs amplitudes from the basal holding current of each train (Fig. 4C, S3E;
399 statistics Table S4). Evolution of summed eIPSCs amplitudes during 50 Hz trains was significantly
400 different in eGFP- or eGFP+ neurons for both normalized amplitudes ($P = 4.90 \cdot 10^{-7}$, Fig. 4C) and
401 raw amplitudes ($P = 4.12 \cdot 10^{-8}$, Fig. S3E).
402 Amplitudes of summated eIPSCs significantly increased during 50 Hz trains in eGFP- neurons
403 ($P_{normalized} = 1.15 \cdot 10^{-5}$, Fig. 3E; $P_{raw} = 3.98 \cdot 10^{-10}$, Fig. S3E). At the asymptote, the increase in raw
404 amplitude was of 123.33 pA and represented an increase by 2.29 folds of the normalized

amplitudes. Importantly, only 86.5 % of the asymptotic value was reached at the end of the train (i.e. 11th eIPSC) suggesting that further summation was still possible with longer lasting trains. In eGFP+ neurons, no significant increase was detected for normalized summed eIPSCs ($P_{normalized}$ = 0.076, Fig. 4C) but raw summated eIPSCs significantly increased during 50 Hz trains (P_{raw} = $0.67 \cdot 10^{-3}$, Fig. S3E). In these neurons, the increase in raw summed amplitude was of 44.47 pA and 95 % of the asymptotic value was reached before the 6th eIPSC indicating that maximal summation is reached with few eIPSCs.

This difference between eGFP- and eGFP+ neurons in eIPSCs-summation during 50 Hz trains was not caused by differences in deactivation kinetics of isolated eIPSCs since these were similar in eGFP- and eGFP+ neurons (see above).

These data indicated that GABAergic connections onto eGFP- and eGFP+ neurons displayed different characteristics of short-term plasticities under high frequency activity: connections onto eGFP+ neurons showed strong depression and limited summation whereas connections onto eGFP- neurons showed no depression and large summation.

Distinct short-term plasticity in simultaneously recorded eGFP- and eGFP+ neurons.

We next defined whether connections from a given presynaptic neuron displayed distinct short-term plasticities when the postsynaptic neuron was eGFP- or eGFP+. To this end, we performed simultaneous recordings of eGFP- and eGFP+ neurons and searched for a presynaptic neuron connecting the recorded ones. For each pair of neuron, we substracted the normalized eIPSCs amplitudes recorded on eGFP+ neurons from those recorded on eGFP- neurons (Fig. 5).

For both 5 Hz and 50 Hz trains, the relative eIPSCs amplitude difference was significantly larger than zero ($P_{5Hz} = 1.26 \cdot 10^{-5}$, n = 6 pairs; $P_{50Hz} = 6.21 \cdot 10^{-6}$, n = 4 pairs, Table S7), indicating that

eIPSCs recorded in eGFP+ neurons depressed relatively to eIPSCs simultaneously recorded in eGFP- neurons.

These data indicated that synapses involving the same presynaptic neuron expressed postsynaptic-target specific plasticities.

Target-specific short-term plasticity involving $GABA_B$ receptors

We next assessed whether the short-term plasticity of GABAergic connections onto LII neurons may involve $GABA_B$ receptors activated by synaptically released GABA (Fig. 6, S7, statistics Table S8). The protocols of 10 trains of stimulations used in the previous experiments were applied twice, i.e. before and during bath application of 10 µM CGP55845, a $GABA_B$ receptors antagonist. First, trains at 5 Hz were repeated every 20 s whereas trains at 50 Hz were repeated every 60 s. When evolution of raw eIPSCs amplitudes was considered, no significant effects of CGP55845 were detected during trains at 5 and 50 Hz in neither eGFP- nor eGFP+ neurons ($P_{eGFP-,\ 5\ Hz} = 0.892$, n = 6; $P_{eGFP-,\ 50\ Hz} = 0.571$, n = 12; $P_{eGFP+,\ 5\ Hz} = 0.881$, n = 8; $P_{eGFP+,\ 50\ Hz} = 0.448$; Fig. S7B, E, H, K, N), indicating that $GABA_B$ receptors were not tonically controlling these connections under these conditions.

Since $GABA_B$ receptors may be activated in a phasic manner by the GABA released during the train of activity, we also analyzed effects of CGP55845 on eIPSCs amplitudes normalized to the firsts eIPSCs of the control trains (Fig. 6, S7, Table S8). Normalized eIPSCs recorded in eGFP- neurons were not modified in presence of CGP55845 during both trains at 5 Hz and at 50 Hz ($P_{eGFP-,\ 5\ Hz} = 0.900$, n = 6; $P_{eGFP-,\ 50\ Hz} = 0.232$, n = 12, Fig. 6A, B). Interestingly, in presence of CGP55845, amplitudes of normalized eIPSCs recorded in eGFP+ neurons during trains at 5 Hz were significantly increased by 38 % with respect to control trains ($P = {}_{eGFP+,\ 5\ Hz} = 1.11 \cdot 10^{-10}$, n =

8, Fig. 6C). A weak effect of CGP55845 was observed during trains at 50 Hz ($P_{eGFP+,\ 50\ Hz} = 6.05 \cdot 10^{-3}$, n = 6, Fig. 6D).

Since trains at 5 Hz were repeated every 20 s and trains at 50 Hz every 60 s, the longer delay for 50 Hz trains may be involved in the lack of CGP55845 effect at this frequency.

Nevertheless, CGP55845 had no effect when trains at 50 Hz were repeated every 20 s (P = 0.330; n = 7, Fig. 6E) indicating that the effect of CGP55845 was not depending on the delay between trains.

Importantly, during trains at 50 Hz repeated every 20s, control eIPSCs amplitudes were larger that during protocols repeated every 60 s ($P = 2.75 \cdot 10^{-9}$), and similar to amplitudes recorded in presence of CGP55845 during trains at 5 Hz repeated every 20 s (P = 0.380). This suggested that facilitating mechanisms engaged at 50 Hz might have overcome an inhibition by $GABA_B$ receptors (compare amplitudes Fig. 6D and 6E).

These results indicated that under our experimental conditions, $GABA_B$ receptors are involved in a phasic modulation of GABAergic connections between LII neurons. This involvement of $GABA_B$ receptors is target-specific, it only occurs at synapses between two GABAergic neurons and at low stimulation frequency (i.e. at 5 Hz).

Target-specific and frequency dependent tonic inhibition involving adenosine A1 receptors

Since synaptic vesicles contain ATP which can be rapidly hydrolyzed into adenosine by extracellular ectonucleotidases [12], we checked whether the short-term plasticity of GABAergic connections onto LII neurons might involve the activation of adenosine A1 receptors (Fig. 7, S8, statistics Table S8). Protocols of 10 trains of stimulations as described previously were applied twice: before and during bath application of 10 µM DPCPX, an antagonist of A1 receptors.

In eGFP- neurons (Fig. 7A-C), DPCPX significantly increased raw eIPSCs amplitudes during trains at 5 Hz repeated every 20 s ($P_{eGFP-,\ 5\ Hz} = 6.28 \cdot 10^{-16}$, n = 9, Fig. 7A) and trains at 50 Hz repeated every 20 s ($P_{eGFP-,\ 50\ Hz} = 2.40 \cdot 10^{-3}$, n = 9, Fig. 7C) but not during trains at 50 Hz repeated every 60 s ($P_{eGFP-,\ 50\ Hz} = 0.119$, n = 7, Fig, 7B). In these neurons, no effect of DPCPX was detected on eIPSCs amplitudes normalized to the firsts eIPSCs of the control trains (Fig. S8), neither at 5 Hz every 20 s ($P_{eGFP-,\ 5\ Hz} = 0.777$, n = 9, Fig. S8C), nor at 50 Hz every 20 s ($P_{eGFP-,\ 50\ Hz} = 0.050$, n = 9, Fig. S8I), nor at 50 Hz every 60 s ($P_{eGFP-,\ 50\ Hz} = 0.600$, n = 7, Fig. S8F). Effects on raw but not normalized amplitudes indicated that adenosine tonically controlled GABAergic connections onto eGFP- neurons. This tonic control was only engaged when trains were repeated every 20 s and not every 60 s indicating that the tone of adenosine controlling GABAergic connections onto eGFP- neurons was linked to the activity of these synapses.

In eGFP+ neurons (Fig. 7D-E), DPCPX increased raw eIPSCs amplitudes during both trains at 5 Hz repeated every 20 s ($P_{eGFP+,\ 5\ Hz} = 1.56 \cdot 10^{-2}$, n = 9, Fig. 7D) and trains at 50 Hz repeated every 60 s ($P_{eGFP+,\ 50\ Hz} = 3.70 \cdot 10^{-2}$, n = 7, Fig. 7E). At both frequencies, the effect of DPCPX on eGFP+ neurons was statistically significant (p-value < 0.05), but the hypothesis of a difference did not unambiguously correspond to the most parsimonious explanation of the data (only AIC but not AICc was lower, see Table S8). In these eGFP+ neurons, no effect of DPCPX was detected on eIPSCs amplitudes normalized to the firsts eIPSCs of the control trains (Fig. S8) at 5 Hz every 20 s ($P_{eGFP+,\ 5\ Hz} = 0.191$, n = 9, Fig. S8L), but a weak effect was detected at 50 Hz every 60 s ($P_{eGFP+,\ 50\ Hz} = 3.70 \cdot 10^{-2}$, n = 7, Fig. S8O). Effects on raw but not normalized amplitudes indicated that adenosine tonically controlled GABAergic connections onto eGFP+ neurons. On these neurons, effect of adenosine was kept when trains were repeated every 60 s.

Interestingly, the tonic control by adenosine was significantly larger on connections onto eGFP- neurons than on connections onto eGFP+ neurons ($P = 2.73 \cdot 10^{-8}$; Fig. 7F, Fig. 7F). The average increase in amplitude during 5 Hz trains was of 47.3 ± 2.9 pA in eGFP- neurons whereas is was of 15.8 ±1.5 pA in eGFP+ neurons.

These data indicated that A1 receptors could tonically inhibit GABAergic connections in LII. This tonic inhibition was stronger on connections onto eGFP- neurons. In these neurons, this tonic control was only engaged when trains were repeated at short intervals.

DISCUSSION

Short-term plasticity is of major importance in information processing in sensory systems where the average number of spikes per unit of time encodes the intensity of adequate stimuli [1; 2; 7; 51]. Using mice expressing eGFP under the control of the GAD65 promoter, we demonstrate that LII GABAergic connections onto putative inhibitory neurons (eGFP+) display different short-term plasticities than those onto putative excitatory neurons (eGFP-). Importantly, in the transgenic mice we used, ~80% of LII eGFP+ neurons were shown to be GABA-immunopositive and ~60% of GABA-immunopositive neurons express eGFP [10]. Therefore, eGFP+ neurons mainly represent GABAergic neurons, and eGFP- neurons excitatory neurons, although the matching is not perfect. This may however partly explain the larger data dispersion observed in eGFP- neurons (e.g. Fig. S4BD).

Nevertheless, the strong difference in short-term plasticity we observed when comparing eGFP- and eGFP+ neurons will probably have an impact on the excitation/inhibition balance within LII networks, and affect the processing of nociceptive information within the dorsal horn.

519

520 **Action-potential firing patterns**

521 Most of eGFP+ neurons we recorded from displayed a tonic action-potential firing pattern.
522 Other groups have reported this firing type in a majority or in a large proportion of LII neurons
523 identified as inhibitory by immunohistochemistry [52], expression of GAD67 [11], GAD65 [10; 24],
524 other genetic markers [18] or assumed from their morphology [16]. A very low proportion of
525 tonic-firing neurons has nevertheless been recorded in a single study in GAD67+ neurons [19].
526 We mostly recorded putative excitatory neurons displaying non-tonic firing, as did other groups
527 [16; 52]. Nevertheless, in our experiments, eGFP- neurons were mostly IB, whereas in the same
528 transgenic line these neurons mostly displayed a delayed firing [10]. Such difference may be
529 linked to distinct intracellular composition as well as distinct initial holding potential as it has
530 already been shown in lamina II [52]. Our data also indicate that both eGFP- and eGFP+ neurons
531 can fire at 50 Hz, and GABAergic neurons reliably trigger eIPSCs during stimulations at this
532 frequency.

533

534 **Inhibitory connections between LII interneurons**

535 Local inhibitory connections between LII neurons are mostly GABAergic, glycinergic transmission
536 occurring in only 1 / 15 inhibitory contacts recorded by Lu and Perl [33], and possibly in 1 / 3
537 inhibitory contacts recorded by Labrakakis et al. [27]. We therefore focused on GABAergic
538 connections since we aimed at examining the short-term plasticity of inhibitory connections
539 between LII neurons. Interestingly, spontaneously active inhibitory connections are dominated
540 by GABAergic transmission in most LIIo neurons, whether these are dominated by glycinergic
541 transmission in most neurons at laminae IIi/III border [48], glycinergic connections onto LII

neurons most likely originating from neurons the cell bodies of which are localized in other laminae.

Paired-pulse plasticity

During paired-pulse stimulation experiments at short ISIs, GABAergic connections onto eGFP- neurons preferentially facilitated whereas, at long ISIs, GABAergic connections onto eGFP+ neurons preferentially depressed. In primary cultures of rat laminae I-III, paired-pulse inhibition of GABAergic eIPSCs was preferentially observed (84%), but facilitation occasionally occurred (16%) [20]. Inhibitory eIPSPs in laminae II-V of Syrian hamsters, with no distinction between GABAergic and glycinergic transmissions, preferentially displayed facilitation [53]. These facilitating connections may correspond to glycinergic eIPSPs since LII glycinergic synapses display strong paired-pulse facilitation for 50 ms ISIs [24]. Thus, in LII, inhibitory connections showing paired-pulse facilitation may preferentially involve GABAergic synapses onto excitatory neurons, or glycinergic connections onto inhibitory neurons. In the dorsal-horn, paired-pulse depression of glycinergic eIPSCs has previously been shown in rat lamina I, with a maximal depression at ISIs of 150-200 ms and involving $GABA_B$ autoreceptors [8].

Frequency-dependent STP

Our results indicate that GABAergic connections onto eGFP+ neurons strongly depress during trains of activity at both low (5 Hz) and high (50 Hz) frequency. In these neurons, trains at high frequency induce a larger depression reaching its maximum faster than during trains at low frequency. By contrast, GABAergic connections onto eGFP- neurons do not depress, allowing summated eIPSCs to reach larger amplitudes at high frequency.

We have reported previously that trains at 2.5 Hz induced a depression of eIPSCs in primary cultures of superficial dorsal-horn neurons from rats [20]. During 10 Hz stimulations, either a depression or a facilitation of eIPSPs were recorded in laminae II-V of Syrian hamsters [53]. With 20 Hz stimulations, eIPSCs onto GABAergic interneurons in LII of adult mice showed a facilitation during the first train, and a depression during subsequent trains [27]. Although in eGFP+ neurons we observed a tendency of such a facilitation-depression switch it was not statistically significant (Fig. S6), suggesting that the facilitation described by other studies may have involved a glycinergic component which has been shown to display a potentiation in LII neurons in response to 2 Hz stimulations [24]. Interestingly, we observed a facilitation-depression switch for the second eIPSCs during repeated trains at 50 Hz in eGFP- neurons (Fig. S6) suggesting that the facilitation observed in eGFP- neurons during paired-pulse stimulation at short intervals is replaced by other types of plasticities during repeated trains of stimulation at 50 Hz. Such combination of short-term facilitation and depression at different repetitions, frequencies and time scales have been observed in other structures and may be relatively common [3].

Interestingly, in recordings performed at room temperature, GABAergic eIPSCs recorded in eGFP+ neurons display slower decay kinetics than those recorded in eGFP- neurons [28]. Such slower kinetic would allow a better summation of overlapping eIPSCS. Nevertheless, in our conditions, eIPSCs kinetics were similar in eGFP+ and eGFP- neurons. Moreover, at high frequency, summated eIPSCs in eGFP- neurons reached larger amplitudes than summated eIPSCs in eGFP+ neurons, ruling out an involvement of different decay kinetics to explain a higher degree of summation of eIPSCs in eGFP- neurons.

Modulation by $GABA_B$ and A1 receptors

Our results indicate that GABAergic connections onto LII neurons can be under a tonic inhibitory control by A1 adenosine receptors. This inhibition is much stronger on connections onto eGFP- neurons than onto eGFP+ neurons. In eGFP- neurons, this inhibition only occurred when trains were delivered at short intervals. This suggests that the tone of adenosine inhibiting these connections is built-up by ongoing activity and decays when activity decreases. These data were consistent with our previous work showing that in cultured dorsal-horn neurons, presynaptic A1 autoreceptors control a subset of GABAergic synapses in an activity-dependent manner [20]. Tonic inhibition by adenosine receptors is not restricted to inhibitory transmission, glutamatergic synapses in LII are also under an inhibitory tone of adenosine, even under low electrical activity within the network [49].

Whereas inhibition of GABAergic connections by A1 receptors was tonic, we showed that $GABA_B$ receptors can be engaged in a phasic depression of GABAergic eIPSCs during trains of activity. This depression involving $GABA_B$ receptors is target-specific: occurring only in connections onto eGFP+ neurons. Interestingly, although $GABA_B$ receptors-mediated inhibition was phasic (it developed during trains), it was only seen when trains were applied at both low-frequency and short intervals (5 Hz, 20 s). This suggests that this inhibition is activity-dependent, but that underlying inhibitory mechanisms might have been surmounted by facilitation occurring during during trains at high-frequency (compare amplitudes Fig. 6D and 6E).

These results were consistent with previous work showing that presynaptic $GABA_B$ receptors decrease inhibitory synaptic transmission in the superficial dorsal-horn [8; 15; 20], and that a tone of GABA activating $GABA_B$ receptors can occur in the dorsal-horn under various conditions [14; 31; 35; 42].

Interestingly, intrathecal administration of $GABA_B$ and A1 agonists have antinociceptive effects [21; 45; 46] which may involve the types of modulation of short-term plasticity described in the present work.

Impact of frequency and target-specific STPs of GABAergic connections onto LII neurons.

GABAergic connections onto inhibitory or excitatory neurons display very distinct frequency-dependent STPs which can engage target-specific G-protein coupled receptors when bursts of activity occur at short intervals. Similar differential STPs involving synapses contacting excitatory and inhibitory neurons have been described in other structures of the central nervous system and have been shown to directly impact the dynamic properties of networks and their excitation/inhibition balance [4; 5; 25; 32; 36; 40; 41]. Therefore, these synapse-specific short-term plasticities and their modulation under various levels of activity are of crucial importance to understand information processing by a network receiving frequency-coded information from the periphery.

At low frequency, corresponding to the activity at low intensity of sensory stimulation under basal physiological conditions, the inhibitory control onto putative excitatory neurons remains constant whereas it depresses onto putative inhibitory neurons. At high frequency, the inhibitory control is increased by summation onto excitatory neurons whereas it remains constant onto inhibitory neurons. Since the latter fire action-potentials in a tonic manner, they are expected to be able to follow higher frequency of excitatory inputs. Therefore, in basal physiological conditions, both STP and firing properties of inhibitory interneurons of LII might concur to favor inhibitory controls of nociceptive information, particularly at high intensity of sensory

stimulation. Hence, the short-term plasticities within this network as well as their modulation by A1 and $GABA_B$ receptors might represent interesting targets in pain-alleviating strategies.

Conflict of interest statement

The authors declare no competing financial interests.

Acknowledgements

We thank Catherine Moreau and Chantal Fitterer for excellent technical assistance and Jean-Luc Rodeau for his help in statistical analysis. This work was supported by Centre National de la Recherche Scientifique, Université de Strasbourg, and the French National Research agency (ANR) contract ANR-17-EURE-0022. LC was supported by EURIDOL Graduate School of Pain, Neuropole Strasbourg, and Société Française d'Etude et de Traitement de la Douleur (SFETD).

References

[1] Adrian ED. The recovery process of excitable tissues: Part I. J Physiol 1920;54(1-2):1-31.

[2] Adrian ED, Zotterman Y. The impulses produced by sensory nerve endings: Part 3. Impulses set up by Touch and Pressure. J Physiol 1926;61(4):465-483.

[3] Anwar H, Li X, Bucher D, Nadim F. Functional roles of short-term synaptic plasticity with an emphasis on inhibition. Curr Opin Neurobiol 2017;43:71-78.

[4] Bartley AF, Dobrunz LE. Short-term plasticity regulates the excitation/inhibition ratio and the temporal window for spike integration in CA1 pyramidal cells. Eur J Neurosci 2015;41(11):1402-1415.

[5] Buonomano DV. Decoding temporal information: A model based on short-term synaptic plasticity. J Neurosci 2000;20(3):1129-1141.

[6] Buonomano DV. The biology of time across different scales. Nat Chem Biol 2007;3(10):594-597.

[7] Campero M, Serra J, Ochoa JL. C-polymodal nociceptors activated by noxious low temperature in human skin. J Physiol 1996;497 (Pt 2):565-572.

[8] Chery N, De Koninck Y. GABA(B) receptors are the first target of released GABA at lamina I inhibitory synapses in the adult rat spinal cord. J Neurophysiol 2000;84(2):1006-1011.

[9] Cordero-Erausquin M, Coull JA, Boudreau D, Rolland M, De Koninck Y. Differential maturation of GABA action and anion reversal potential in spinal lamina I neurons: impact of chloride extrusion capacity. J Neurosci 2005;25(42):9613-9623.

[10] Cui L, Kim YR, Kim HY, Lee SC, Shin HS, Szabo G, Erdelyi F, Kim J, Kim SJ. Modulation of synaptic transmission from primary afferents to spinal substantia gelatinosa neurons by group III mGluRs in GAD65-EGFP transgenic mice. J Neurophysiol 2011;105(3):1102-1111.

[11] Daniele CA, MacDermott AB. Low-threshold primary afferent drive onto GABAergic interneurons in the superficial dorsal horn of the mouse. J Neurosci 2009;29(3):686-695.

[12] Dunwiddie TV, Diao L, Proctor WR. Adenine nucleotides undergo rapid, quantitative conversion to adenosine in the extracellular space in rat hippocampus. J Neurosci 1997;17(20):7673-7682.

[13] Froemke RC, Merzenich MM, Schreiner CE. A synaptic memory trace for cortical receptive field plasticity. Nature 2007;450(7168):425-429.

[14] Fukuhara K, Katafuchi T, Yoshimura M. Effects of baclofen on mechanical noxious and innocuous transmission in the spinal dorsal horn of the adult rat: in vivo patch-clamp analysis. Eur J Neurosci 2013;38(10):3398-3407.

[15] Grudt TJ, Henderson G. Glycine and GABAA receptor-mediated synaptic transmission in rat substantia gelatinosa: inhibition by mu-opioid and GABAB agonists. J Physiol 1998;507 (Pt 2):473-483.

[16] Grudt TJ, Perl ER. Correlations between neuronal morphology and electrophysiological features in the rodent superficial dorsal horn. J Physiol 2002;540(Pt 1):189-207.

[17] Guan Y. Spinal cord stimulation: neurophysiological and neurochemical mechanisms of action. Curr Pain Headache Rep 2012;16(3):217-225.

[18] Hantman AW, van den Pol AN, Perl ER. Morphological and physiological features of a set of spinal substantia gelatinosa neurons defined by green fluorescent protein expression. J Neurosci 2004;24(4):836-842.

[19] Heinke B, Ruscheweyh R, Forsthuber L, Wunderbaldinger G, Sandkuhler J. Physiological, neurochemical and morphological properties of a subgroup of GABAergic spinal lamina II neurones identified by expression of green fluorescent protein in mice. J Physiol 2004;560(Pt 1):249-266.

694 [20] Hugel S, Schlichter R. Convergent control of synaptic GABA release from rat dorsal horn
695 neurones by adenosine and GABA autoreceptors. J Physiol 2003;551(Pt 2):479-489.
696 [21] Jacobson KA, Gao ZG. Adenosine receptors as therapeutic targets. Nat Rev Drug Discov
697 2006;5(3):247-264.
698 [22] Jensen MP, Brownstone RM. Mechanisms of spinal cord stimulation for the treatment of pain:
699 Still in the dark after 50 years. Eur J Pain 2019;23(4):652-659.
700 [23] Kato G, Kawasaki Y, Ji RR, Strassman AM. Differential wiring of local excitatory and inhibitory
701 synaptic inputs to islet cells in rat spinal lamina II demonstrated by laser scanning
702 photostimulation. J Physiol 2007;580(Pt.3):815-833.
703 [24] Kloc ML, Pradier B, Chirila AM, Kauer JA. NMDA receptor activation induces long-term
704 potentiation of glycine synapses. PLoS One 2019;14(9):e0222066.
705 [25] Klyachko VA, Stevens CF. Excitatory and feed-forward inhibitory hippocampal synapses work
706 synergistically as an adaptive filter of natural spike trains. PLoS Biol 2006;4(7):e207.
707 [26] Kuhlman SJ, Olivas ND, Tring E, Ikrar T, Xu X, Trachtenberg JT. A disinhibitory microcircuit
708 initiates critical-period plasticity in the visual cortex. Nature 2013;501(7468):543-546.
709 [27] Labrakakis C, Lorenzo LE, Bories C, Ribeiro-da-Silva A, De Koninck Y. Inhibitory coupling
710 between inhibitory interneurons in the spinal cord dorsal horn. Mol Pain 2009;5:24.
711 [28] Labrakakis C, Rudolph U, De Koninck Y. The heterogeneity in GABAA receptor-mediated
712 IPSC kinetics reflects heterogeneity of subunit composition among inhibitory and
713 excitatory interneurons in spinal lamina II. Front Cell Neurosci 2014;8:424.
714 [29] Letzkus JJ, Wolff SB, Meyer EM, Tovote P, Courtin J, Herry C, Luthi A. A disinhibitory
715 microcircuit for associative fear learning in the auditory cortex. Nature
716 2011;480(7377):331-335.
717 [30] Light AR, Perl ER. Reexamination of the dorsal root projection to the spinal dorsal horn
718 including observations on the differential termination of coarse and fine fibers. J Comp
719 Neurol 1979;186(2):117-131.
720 [31] Lin Q, Peng YB, Willis WD. Role of GABA receptor subtypes in inhibition of primate
721 spinothalamic tract neurons: difference between spinal and periaqueductal gray inhibition.
722 J Neurophysiol 1996;75(1):109-123.
723 [32] Lovett-Barron M, Turi GF, Kaifosh P, Lee PH, Bolze F, Sun XH, Nicoud JF, Zemelman BV,
724 Sternson SM, Losonczy A. Regulation of neuronal input transformations by tunable
725 dendritic inhibition. Nat Neurosci 2012;15(3):423-430, S421-423.
726 [33] Lu Y, Perl ER. A specific inhibitory pathway between substantia gelatinosa neurons receiving
727 direct C-fiber input. J Neurosci 2003;23(25):8752-8758.

728 [34] Lu Y, Perl ER. Modular organization of excitatory circuits between neurons of the spinal
729 superficial dorsal horn (laminae I and II). J Neurosci 2005;25(15):3900-3907.
730 [35] Malan TP, Mata HP, Porreca F. Spinal GABA(A) and GABA(B) receptor pharmacology in a
731 rat model of neuropathic pain. Anesthesiology 2002;96(5):1161-1167.
732 [36] Moreno A, Morris RGM, Canals S. Frequency-Dependent Gating of Hippocampal-Neocortical
733 Interactions. Cereb Cortex 2016;26(5):2105-2114.
734 [37] Motanis H, Seay MJ, Buonomano DV. Short-Term Synaptic Plasticity as a Mechanism for
735 Sensory Timing. Trends Neurosci 2018;41(10):701-711.
736 [38] Motulsky HJ, Christopoulos A. Fitting Models to Biological Data Using Linear and Nonlinear
737 Regression. San Diego: GraphPad Software Inc., 2003.
738 [39] Polgar E, Durrieux C, Hughes DI, Todd AJ. A quantitative study of inhibitory interneurons in
739 laminae I-III of the mouse spinal dorsal horn. PLoS One 2013;8(10):e78309.
740 [40] Pouille F, Scanziani M. Routing of spike series by dynamic circuits in the hippocampus.
741 Nature 2004;429(6993):717-723.
742 [41] Royer S, Zemelman BV, Losonczy A, Kim J, Chance F, Magee JC, Buzsaki G. Control of
743 timing, rate and bursts of hippocampal place cells by dendritic and somatic inhibition. Nat
744 Neurosci 2012;15(5):769-775.
745 [42] Salio C, Merighi A, Bardoni R. GABAB receptors-mediated tonic inhibition of glutamate
746 release from Abeta fibers in rat laminae III/IV of the spinal cord dorsal horn. Mol Pain
747 2017;13:1744806917710041.
748 [43] Santos SF, Luz LL, Szucs P, Lima D, Derkach VA, Safronov BV. Transmission efficacy and
749 plasticity in glutamatergic synapses formed by excitatory interneurons of the substantia
750 gelatinosa in the rat spinal cord. PLoS One 2009;4(11):e8047.
751 [44] Santos SF, Rebelo S, Derkach VA, Safronov BV. Excitatory interneurons dominate sensory
752 processing in the spinal substantia gelatinosa of rat. J Physiol 2007;581(Pt 1):241-254.
753 [45] Sawynok J, LaBella FS. On the involvement of GABA in the analgesia produced by baclofen,
754 muscimol and morphine. Neuropharmacology 1982;21(5):397-403.
755 [46] Schenone S, Brullo C, Musumeci F, Bruno O, Botta M. A1 receptors ligands: past, present
756 and future trends. Curr Top Med Chem 2010;10(9):878-901.
757 [47] Spiess AN, Neumeyer N. An evaluation of R2 as an inadequate measure for nonlinear models
758 in pharmacological and biochemical research: a Monte Carlo approach. BMC Pharmacol
759 2010;10:6.
760 [48] Takazawa T, MacDermott AB. Synaptic pathways and inhibitory gates in the spinal cord
761 dorsal horn. Ann N Y Acad Sci 2010;1198:153-158.

[49] Tian L, Ji G, Wang C, Bai X, Lu Y, Xiong L. Excitatory synaptic transmission in the spinal substantia gelatinosa is under an inhibitory tone of endogenous adenosine. Neurosci Lett 2010;477(1):28-32.

[50] Todd AJ. Plasticity of inhibition in the spinal cord. Handb Exp Pharmacol 2015;227:171-190.

[51] Torebjork HE, Hallin RG. Responses in human A and C fibres to repeated electrical intradermal stimulation. J Neurol Neurosurg Psychiatry 1974;37(6):653-664.

[52] Yasaka T, Tiong SY, Hughes DI, Riddell JS, Todd AJ. Populations of inhibitory and excitatory interneurons in lamina II of the adult rat spinal dorsal horn revealed by a combined electrophysiological and anatomical approach. Pain 2010;151(2):475-488.

[53] Zhang W, Schneider SP. Short-term modulation at synapses between neurons in laminae II-V of the rodent spinal dorsal horn. J Neurophysiol 2011;105(6):2920-2930.

[54] Zheng J, Lu Y, Perl ER. Inhibitory neurones of the spinal substantia gelatinosa mediate interaction of signals from primary afferents. J Physiol 2010;588(Pt 12):2065-2075.

Figure 1. Action-potential firing patterns in eGFP+ and eGFP- neurons.

A. example of a tonic-firing eGFP+ neuron (left) and of an initial bursting eGFP- neuron (right). **B.** A majority of eGFP+ neurons were of tonic-firing type (Tonic) whereas a majority of eGFP- neurons were of initial bursting type (IB). Proportions of firing patterns were significantly different in eGFP+ and eGFP- neurons (Fisher's exact test, $P = 6.3 \cdot 10^{-6}$; n = 67 eGFP+ neurons and 61 eGFP- neurons). **C.** Instantaneous firing frequency in 100 ms bins in response to 1 s-long 80 pA current injections in eGFP- IB neurons (left) and eGFP+ Tonic neurons (right). **D.** Spiking in an eGFP- (left) and an eGFP+ (right) neuron during a 50 Hz train of simulated EPSCs. **E.** Probability of action-potential spiking per simulated EPSCs in eGFP- neurons (n = 7) and eGFP+ neurons (n = 4).

Figure 2. GABAergic IPSCs recorded in eGFP+ and eGFP- neurons.

A. Amplitude of eIPSCs is similar in eGFP+ (green) and eGFP- neurons (blue). **B.** Left: example of eIPSCs recorded in an eGFP+ and an eGFP- neuron (average of 10 eIPSCs; eIPSCs are scaled). Right: Weighted decay time-constant of GABAergic eIPSCs is similar in eGFP+ and eGFP- neurons. **C.** Amplitudes of mIPSCs are similar in eGFP+ and eGFP- neurons. **D.** Proportions of neurons displaying a paired-pulse facilitation (PPR > 1.1), a paired-pulse depression (PPR < 0.9), or no change in PPR (0.9-1.1) at various inter-stimulation intervals (ISIs) in eGFP+ and eGFP- neurons. These proportions are significantly different in eGFP+ and eGFP- neurons (Log-linear analysis; P=0.003). **E.** PPRs as a function of ISIs were significantly different in eGFP+ and eGFP- neurons (Non-linear curve fitting, $P = 7.20 \cdot 10^{-3}$). Curves correspond to fits with monoexponential functions. Numbers beside the points correspond to the number of neurons recorded.

Figure 3. Short-term plasticity of GABAergic connections during trains at 5 Hz.

A. Representative average current trace recorded in an eGFP- neuron (top) and eGFP+ neuron (bottom). **B.** Relative amplitudes of GABAergic eIPSCs recorded in eGFP- and eGFP+ neurons (amplitudes normalized after eIPSCs of rank 1). **C. D.** Changes in eIPSCs amplitudes during the trains remained similar in the first five and the last five trains for connections on both eGFP- (C) and eGFP+ (D) neurons. Results of non-linear regressions used to compare conditions are given as P > 0.5: n.s. and P < 0.001: ***. n = 54 eGFP- and n = 49 eGFP+ neurons. Details of regressions and the corresponding analysis are given in Supplementary Table 1.

Figure 4. Short-term plasticity of GABAergic connections during trains at 50 Hz.

A. Representative average current trace recorded in an eGFP- neuron (left) and eGFP+ neuron (right). **B.** Relative amplitudes of GABAergic eIPSCs recorded in eGFP- and eGFP+ neurons

(amplitudes normalized after eIPSCs of rank 1). **C.** Same data as in B, but with eIPSCs measured from the basal current level before the first eIPSC (summated eIPSCs amplitudes). **D. E.** Changes in eIPSCs amplitudes during the trains remained similar in the first five and the last five trains for connections on both eGFP- (D) and eGFP+ (E) neurons. Results of non-linear regressions used to compare conditions are given as $P > 0.5$: n.s. and $P < 0.001$: ***. n = 27 eGFP- and n = 19 eGFP+ neurons. Details of regressions and the corresponding analysis are given in Supplementary Table 1.

Figure 5. Distinct short-term plasticities in simultaneously recorded eGFP- and eGFP+ neurons. **A.** Short-term plasticity during stimulation trains at 5 Hz. Left: representative average current trace simultaneously recorded in an eGFP- neuron (blue) and eGFP+ neuron (green). Right: for each pair of eGFP- and eGFP+ neuron and for all ranks during the train, the difference in relative eIPSCs amplitude is calculated. This difference is significantly larger than zero indicating that the relative increase in amplitude during the train at 5 Hz is larger in eGFP- than in eGFP+ neurons ($P < 0.001$: ***; n = 6 pairs).

B. Short-term plasticity during stimulation trains at 50 Hz. Left: representative average current trace simultaneously recorded in an eGFP- neuron (blue) and eGFP+ neuron (green). Right: for each pair of eGFP- and eGFP+ neuron and for all ranks during the train, the difference in relative eIPSCs amplitude is calculated. This difference is significantly larger than zero indicating that the relative increase in amplitude during the train at 50 Hz is larger in eGFP- than in eGFP+ neurons ($P < 0.001$: ***; n = 4 pairs). Linear regressions of the data were compared with a linear regression with a slope set at 0 which would correspond to no differences in eIPSCs amplitudes in eGFP- and

834 eGFP+ neurons. Details of regressions and the corresponding analysis are given in Supplementary
835 Table 1.
836
837 **Figure 6. Effect of a $GABA_B$ receptor antagonist on GABAergic eIPSCs during trains of**
838 **stimulations.**
839 **A-E.** Average normalized amplitudes of GABAergic eIPSCs during trains of stimulations at 5 Hz
840 and 50 Hz, before (blue and green) and during bath application of 10 µM CGP55845 (red), a
841 $GABA_B$ receptors antagonist. For each neuron, trains of 11 stimulations were repeated 10 times
842 in control condition and 10 times during bath application of 10 µM CGP55845. The type of neuron
843 recorded (eGFP- or eGFP+), the frequency of stimulation (5 Hz or 50 Hz) and the interval between
844 trains (20 s or 60 s) are given on the top of each panel. **A-B.** CGP55845 had no effect on GABAergic
845 connections onto eGFP- neurons, neither during trains at 5 Hz (A, n = 6 neurons) nor during trains
846 at 50 Hz (B, n = 12 neurons). **C-E.** In eGFP+ neurons CGP55845 significantly increased normalized
847 eIPSCs amplitudes during 5 Hz trains repeated every 20 s (C, n = 8 neurons) but neither during 50
848 Hz trains repeated every 60 s (D, n = 6 neurons) nor 50 Hz trains repeated every 20 s (E, n = 7
849 neurons). Results of non-linear regressions used to compare conditions are given as $P > 0.5$: n.s.,
850 $0.05 < P < 0.01$: *, and $P < 0.001$: ***. Details of regressions and the corresponding analysis are
851 given in Supplementary Table 1.
852
853 **Figure 7. Effect of an A1 adenosine receptor antagonist on GABAergic eIPSCs during trains of**
854 **stimulations**
855 **A-E.** Average raw amplitudes of GABAergic eIPSCs during trains at 5 Hz and 50 Hz before (blue
856 and green) and during bath application of 10 µM DPCPX (pink), an A1 receptor antagonist. For

each neuron, trains of 11 stimulations were repeated 10 times in control condition and 10 times during bath application of DPCPX. The type of neuron recorded (eGFP- or eGFP+), the frequency of stimulation (5 Hz or 50 Hz) and the interval between trains (20 s or 60 s) are given on the top of each panel. **A-C.** In eGFP- neurons, DPCPX significantly increased raw eIPSCs amplitudes during 5 Hz trains repeated every 20 s (A, n = 9 neurons) and 50 Hz trains repeated every 20 s (C, n = 9 neurons) but not during 50 Hz trains repeated every 60 s (B, n = 7 neurons). This indicated a tonic inhibition of GABAergic connections onto eGFP- neurons by adenosine depending on the delay between trains of stimulation. **D-E**. In eGFP+ neurons, DPCPX significantly increased raw eIPSCs amplitudes during 5 Hz trains repeated every 20 s (D, n = 9 neurons) and 50 Hz trains repeated every 60 s (E, n = 7 neurons). This indicated a tonic inhibition of GABAergic connections onto eGFP+ neurons. **F.** Average increase in raw eIPSCs amplitudes in presence of DPCPX with respect to control conditions. For trains at 5 Hz, the increase in amplitude is larger in eGFP- neurons than in eGFP+ neurons. Evolution of eIPSCs amplitudes during trains were compared with non-linear regression. Details of regressions and the corresponding analysis are given in Supplementary Table 1.

Supplementary Figures and table legends

Supplementary figure S1. Data quantification, analysis and statistics.

Stimulation protocols were applied ten times in each neuron and the within-cell average across trials was calculated by averaging eIPSCs amplitudes from these ten repetitions. These within-cell average across ten trials were used for statistical analysis. Non-linear regression analysis was used to analyze changes in eIPSCs amplitudes during stimulation train protocols. To compare two different conditions (e.g. eGFP- vs. eGFP+ or presence/absence of antagonists) data from each

conditions were fitted with Equation 3, either individually (sum of two functions) or pooled (one single function). When the sum of two individual fits provided statistically significant improvements with respect to the fit of pooled data, the two conditions were considered as having distinct effects. To define whether STP was expressed during trains of stimulations, i.e. whether significant changes in amplitude occurred during the train, fits with Equation 3 were compared with linear fits with slope values forced to 0. When fits with Equation 3 provided statistically significant improvements with respect to the linear fit with slope value forced to 0, the connections were considered as displaying a significant STP during the corresponding protocol. Details of all models (number of neurons, degree of freedom, Residual sum of squares, AIC, AICc, BIC) as well as details of model comparison (F, P, differences in AIC, AICc and BIC) are given in Supplementary table 1. Individual data of all neurons were always used for curve fitting and average values were used for illustration.

Supplementary figure S2.

Action-potential firing patterns in eGFP+ (left) and eGFP- (right) neurons.

A majority of eGFP+ neurons were of tonic-firing type (Tonic) whereas a majority of eGFP- neurons were of initial bursting type (n = 67 eGFP+ neurons and 61 eGFP- neurons).

Supplementary figure S3.

Short-term plasticity of GABAergic connections during trains at 5 Hz and 50 Hz.

A. Average raw eIPSCs amplitudes of GABAergic eIPSCs recorded in eGFP- neurons (blue) and eGFP+ neurons (green) during 5 Hz protocols. **B.** Relative amplitudes of GABAergic eIPSCs recorded in eGFP- and eGFP+ neurons (amplitudes normalized after eIPSCs of rank 1, same

neurons as in A). **C.** Average raw eIPSCs amplitudes of GABAergic eIPSCs recorded in eGFP- neurons (blue) and eGFP+ neurons (green) during 50 Hz protocols. **D.** Relative amplitudes of GABAergic eIPSCs recorded in eGFP- and eGFP+ neurons (amplitudes normalized after eIPSCs of rank 1, same neurons as in C). **E. F.** Same data as in C-D, but with eIPSCs measured from the basal current level before the first eIPSC (summated eIPSCs amplitudes). Results of non-linear regressions used to compare conditions are given as $P > 0.5$: n.s. and $P < 0.001$: ***. Details of regressions and the corresponding analysis are given in Supplementary Table 1. For 5 Hz protocols: n = 54 eGFP- and n = 49 eGFP+ neurons. For 50 Hz protocols: n = 27 eGFP- and n = 19 eGFP+ neurons.

Supplementary figure S4. Short-term plasticity of GABAergic connections during trains at 5 Hz and 50 Hz: individual neurons.

Left: Average raw eIPSCs amplitudes of GABAergic eIPSCs. **Right:** Relative amplitudes of GABAergic eIPSCs (amplitudes normalized after eIPSCs of rank 1, same neurons as left).

A-D: train of stimulations at 5 Hz. Same data as in Fig. 3. n = 54 eGFP- and n = 49 eGFP+ neurons.

E-H: trains of stimulations at 50 Hz. Same data as in Fig. 4. n = 27 eGFP- and n = 19 eGFP+ neurons.

A, B, E, F: eIPSCs recorded in eGFP- neurons. **C, D, G, H:** eIPSCs recorded in eGFP+ neurons.

Average amplitudes from individual neurons are in grey.

Supplementary figure S5. Short-term plasticity of GABAergic connections during trains of stimulations at 5 Hz with increased amplitudes of stimulation.

For this experiment, stimulation amplitudes were set at 0.45 mA (versus 0.21 mA on average for all other experiments). **A.** Average raw eIPSCs amplitudes of GABAergic eIPSCs recorded in eGFP-

neurons (blue) and eGFP+ neurons (green). **B.** Relative amplitudes of GABAergic eIPSCs recorded in eGFP- and eGFP+ neurons (amplitudes normalized after eIPSCs of rank 1, same neurons as in A). n = 11 eGFP- and n = 11 eGFP+ neurons.

Evolution of eIPSCs amplitudes during the trains were significantly different in eGFP- and eGFP+ neurons as it was observed with lower amplitudes of stimulation (Fig. 3). This indicated that changes in stimulation efficacy during trains of stimulations were unlikely to influence our results.

Supplementary figure S6. Relative amplitude of rank 2 eIPSCs in the first five and the last five trains.

A. During 5 Hz trains, eIPSC2/eIPSC1 remained similar in the first five and the last five trains for connections on both eGFP- and eGFP+ neurons (P_{eGFP-} = 0.678, P_{eGFP+} = 0.223, Wilcoxon Signed Rank Test for Paired Data). **B.** During 50 Hz trains, eIPSC2/eIPSC1 remained similar in the first five and the last five trains for connections on eGFP+ neurons (P_{eGFP+} = 0.098, Wilcoxon Signed Rank Test for Paired Data), but significantly decreased by 18% for eGFP- neurons (P_{eGFP-} = 0.048, Wilcoxon Signed Rank Test for Paired Data). This suggests that the facilitation observed in eGFP- neurons during paired-pulse stimulation at short intervals (Fig. 2E) is replaced by other types of plasticities during repeated trains of stimulation at 50 Hz.

Supplementary figure S7. Effect of a $GABA_B$ receptor antagonist on GABAergic eIPSCs during 5 Hz and 50 Hz trains.

Average amplitudes of GABAergic eIPSCs during trains at 5 Hz and 50 Hz before (blue and green) and during bath application of 10 µM CGP55845 (orange), a $GABA_B$ receptors antagonist. For each neuron, trains of 11 stimulations were repeated 10 times in control condition and 10 times

during bath application of CGP55845. **A, D, G, J, M.** Type of neuron (eGFP- or eGFP+), frequency of stimulation (5 Hz or 50 Hz) and interval between trains (20 s or 60 s) applied in B-C, E-F, H-I, K-L, N-O, respectively. **B, E, H, K, N.** Average raw eIPSCs amplitudes. **C, F, I, L, O.** Average relative eIPSCs amplitudes. **A-F**: CGP55845 had no effect on GABAergic connections onto eGFP- neurons, neither during trains at 5 Hz (A-C, n = 6 neurons) nor during trains at 50 Hz (D-F n = 12 neurons). **G-O**: in eGFP+ neurons CGP55845 did not changed raw eIPSCs amplitudes (H, K, N), but it significantly increased relative eIPSCs amplitude during 5 Hz trains repeated every 20 s (I, n = 8 neurons), indicating a phasic inhibition involving $GABA_B$ receptors during these trains. Evolution of eIPSCs amplitudes during trains were compared with non-linear regression. Details of regressions and the corresponding analysis are given in Supplementary Table 1. $P > 0.5$: n.s. and $P < 0.001$: ***.

Supplementary figure S8. Effect of an A1 adenosine receptor antagonist on GABAergic eIPSCs during 5 Hz and 50 Hz trains.

Average amplitudes of GABAergic eIPSCs during trains at 5 Hz and 50 Hz before (blue and green) and during bath application of 10 µM DPCPX (pink), an A1 receptor antagonist. For each neuron, trains of 11 stimulations were repeated 10 times in control condition and 10 times during bath application of DPCPX. **A, D, G, J, M.** Type of neuron (eGFP- or eGFP+), frequency of stimulation (5 Hz or 50 Hz) and interval between trains (20 s or 60 s) applied in B-C, E-F, H-I, K-L, N-O, respectively. **B, E, H, K, N.** Average raw eIPSCs amplitudes. **C, F, I, L, O.** Average relative eIPSCs amplitudes. **B, H.** DPCPX significantly increased raw eIPSCs amplitudes recorded in eGFP- neurons during trains at 5 Hz repeated every 20 s (B, n = 9 neurons) and 50 Hz repeated every 20 s (H, n = 9 neurons) but had no effect on raw eIPSCs amplitudes recorded during trains at 50 Hz repeated

every 60 s (E, n = 7 neurons). This indicated a tonic inhibition of GABAergic connections onto eGFP- neurons by adenosine depending on the delay between trains of stimulation. **K, N,** in eGFP+ neurons, DPCPX significantly increased raw eIPSCs amplitudes during 5 Hz trains repeated every 20 s (K) and 50 Hz trains repeated every 60 s (N). This indicated a tonic inhibition of GABAergic connections onto eGFP+ neurons. **C, F, I, L, O** Except during 50 Hz trains repeated every 60 s where a weak significant effect was recorded (O), no effect of DPCPX was detected in relative eIPSCs amplitudes, neither in eGFP- nor in eGFP+ neurons indicating that inhibition involving A1 receptors did not changed during the train. Evolution of eIPSCs amplitudes during trains were compared with non-linear regression. Details of regressions and the corresponding analysis are given in Supplementary Table 1. $P > 0.5$: n.s., $0.05 > P > 0.01$: *, $P < 0.001$: ***.

Supplementary tables 1-7. Data analysis, model comparison and statistics.

The tables correspond to the different figures illustrating the comparisons.

The column **Figure** indicates the panel of the figure illustrating the conditions compared.

In these figures, the averaged eIPSCs amplitudes in the two conditions are illustrated, but statistical analysis were performed using averaged eIPSCs amplitudes of each neurons. These values were calculated by averaging eIPSCs amplitudes of the same rank obtained from reiterations of the protocols. The reiterations used for the average are indicated in the column **Protocol repetition** (usually iterations 1-10). For protocols using trains of stimulations, the **frequency** of stimulations is given (5 Hz or 50 Hz) as well as the time between protocols (20 s or 60 s) in the column **Protocol interval**. The **Type of data** column indicates whether data were averaged raw eIPSCs amplitudes (Raw) or averaged normalized amplitudes (Norm). The **eGFP condition** column indicates whether the data compared were from eGFP- (**-**) or eGFP+ (**+**)

neurons or both (+ and -). The **Drug condition** column indicates whether the data compared were recorded without (**Control**) or with CGP55845 or DPCPX, or both. The **Model** column indicates the two models compared. **N neurons** corresponds to the number of neurons (eGFP- (**-**) or eGFP+ (**+**)). **N obs** corresponds to the number of observations. In experiments with trains of stimulations, the number of observations per neuron and per condition was of 11 for raw data and 10 for normalized data. **k** corresponds to the number of parameters in the model. A1, A2 and A3 are the parameters calculated by non-linear regression (two A1, A2 and A3 are given when a sum of two regressions are used). **SS** is the residual sum of squares calculated with the model. **df** is the degree of freedom of the model. **AIC** is Akaike information criterion; **AICc** is the AIC corrected for small samples; **BIC** is the bayesian information criterion. **F** is the value of the F-distribution of the comparison between the two models. **p** is the corresponding p-value. dAICc is the decrease in AICc provided by the model indicated in that line with respect to the model in the line above. A positive value indicate that the model correspond to the most parsimonious explanation with respect to the model in the line above.

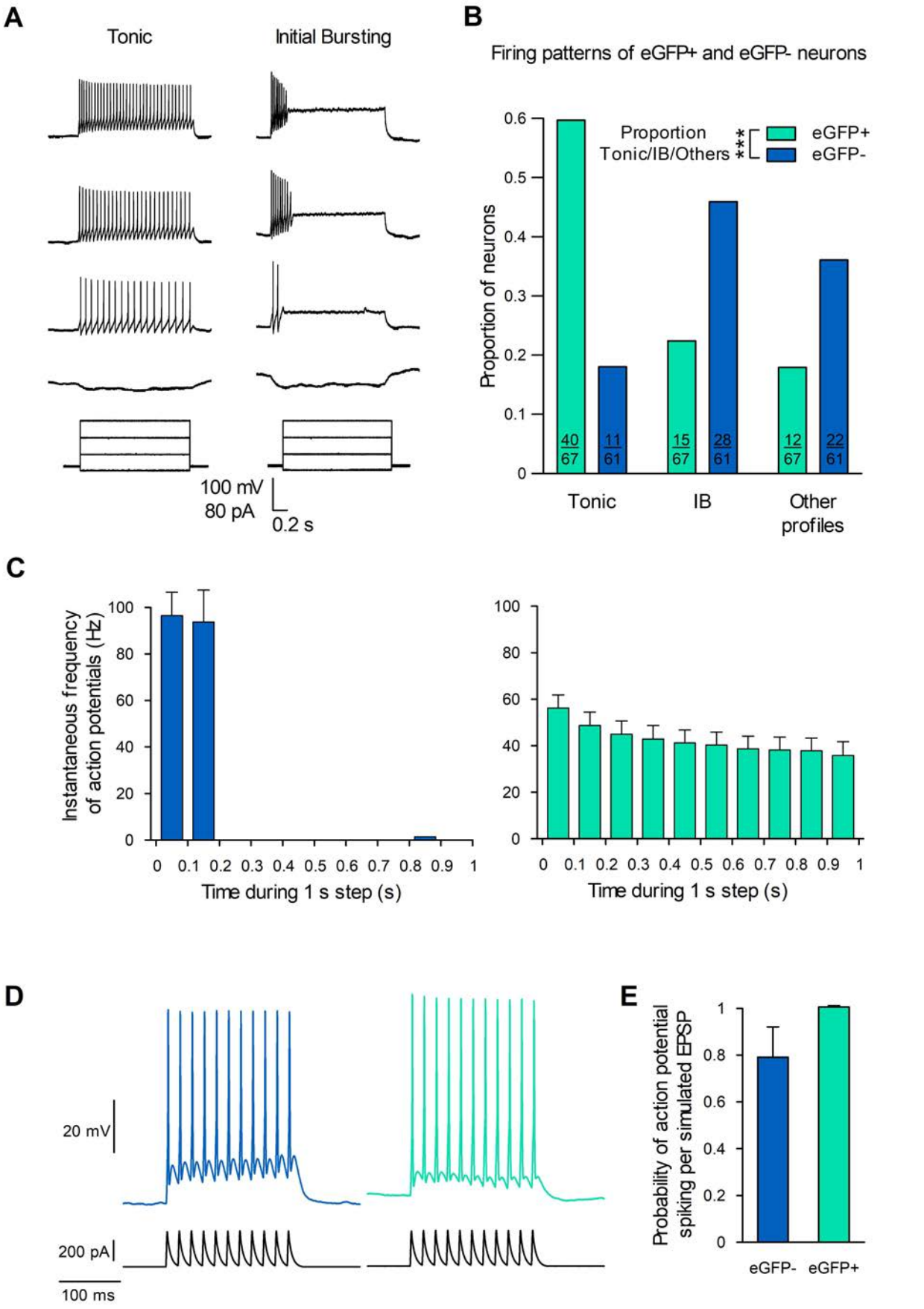
A
Tonic
Initial Bursting
100 mV
80 pA
0.2 s
B
Firing patterns of eGFP+ and eGFP- neurons
Proportion Tonic/IB/Others
***
eGFP+
eGFP-
Proportion of neurons
0.6
0.5
0.4
0.3
0.2
0.1
0
40/67
11/61
15/67
28/61
12/67
22/61
Tonic
IB
Other profiles
C
Instantaneous frequency of action potentials (Hz)
100
80
60
40
20
0
0 0.1 0.2 0.3 0.4 0.5 0.6 0.7 0.8 0.9 1
Time during 1 s step (s)
100
80
60
40
20
0
0 0.1 0.2 0.3 0.4 0.5 0.6 0.7 0.8 0.9 1
Time during 1 s step (s)
D
20 mV
200 pA
100 ms
E
Probability of action potential spiking per simulated EPSP
1
0.8
0.6
0.4
0.2
0
eGFP-
eGFP+

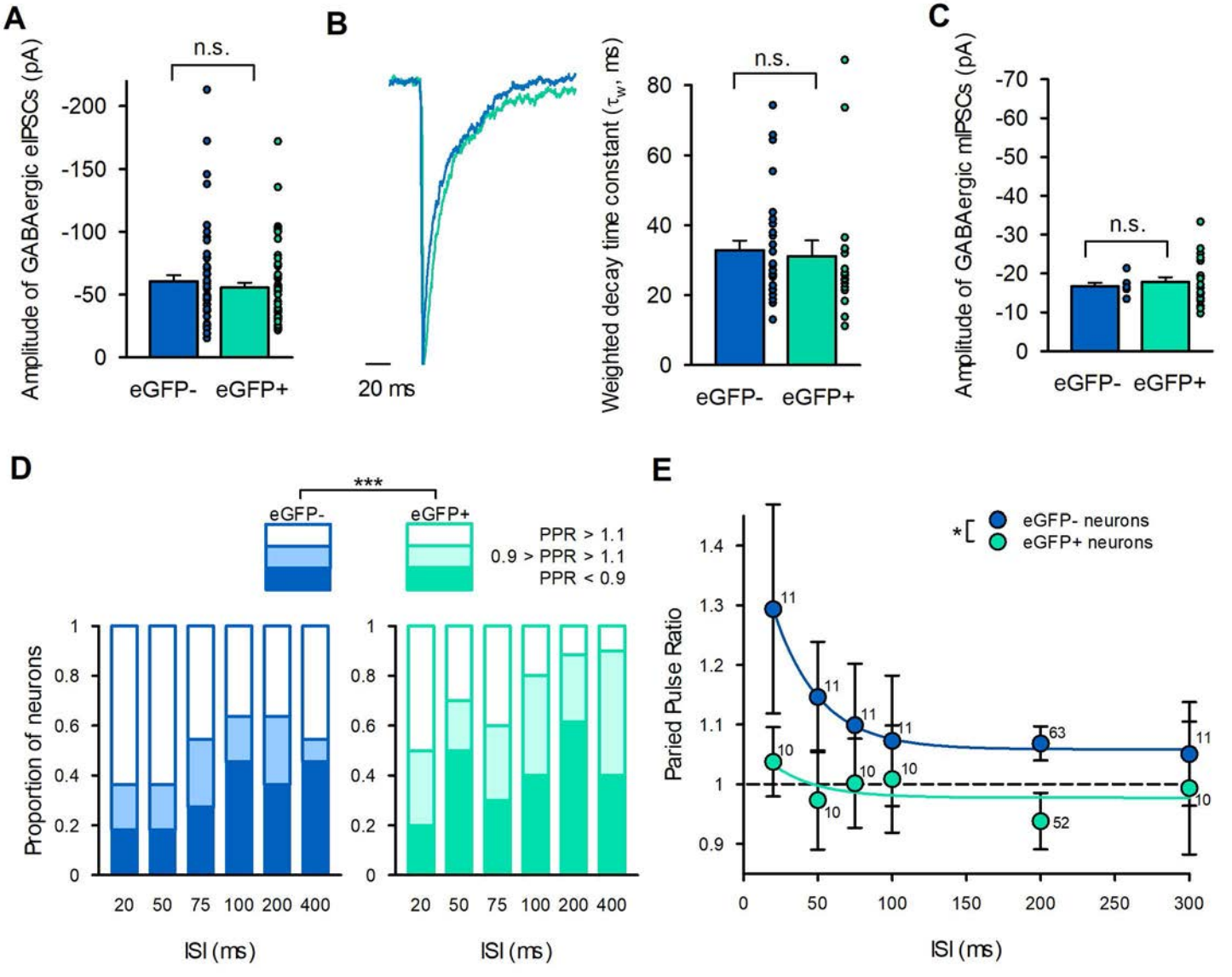
A
n.s.
Amplitude of GABAergic eIPSCs (pA)
-200
-150
-100
-50
0
eGFP-
eGFP+
B
20 ms
n.s.
Weighted decay time constant (τ_w, ms)
80
60
40
20
0
eGFP-
eGFP+
C
n.s.
Amplitude of GABAergic mIPSCs (pA)
-70
-60
-50
-40
-30
-20
-10
0
eGFP-
eGFP+
D
***
eGFP-
eGFP+
PPR > 1.1
0.9 > PPR > 1.1
PPR < 0.9
Proportion of neurons
1
0.8
0.6
0.4
0.2
0
20
50
75
100
200
400
ISI (ms)
E
eGFP- neurons
eGFP+ neurons
Paired Pulse Ratio
1.4
1.3
1.2
1.1
1
0.9
11
10
63
52
0
50
100
150
200
250
300
ISI (ms)

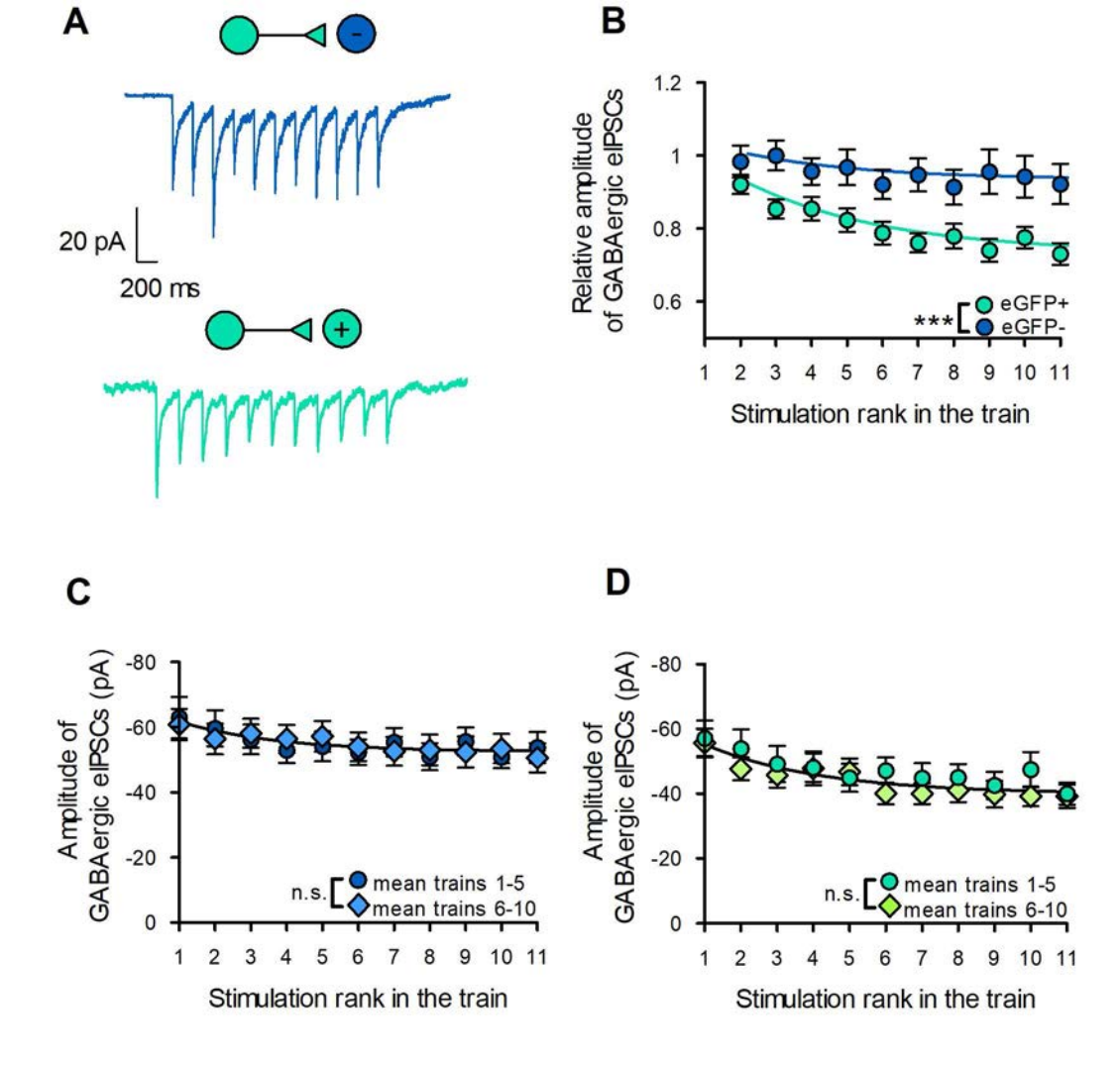
A
20 pA
200 ms
B
Relative amplitude of GABAergic eIPSCs
1.2
1
0.8
0.6
***
eGFP+
eGFP-
1 2 3 4 5 6 7 8 9 10 11
Stimulation rank in the train
C
Amplitude of GABAergic eIPSCs (pA)
-80
-60
-40
-20
0
n.s.
mean trains 1-5
mean trains 6-10
1 2 3 4 5 6 7 8 9 10 11
Stimulation rank in the train
D
Amplitude of GABAergic eIPSCs (pA)
-80
-60
-40
-20
0
n.s.
mean trains 1-5
mean trains 6-10
1 2 3 4 5 6 7 8 9 10 11
Stimulation rank in the train

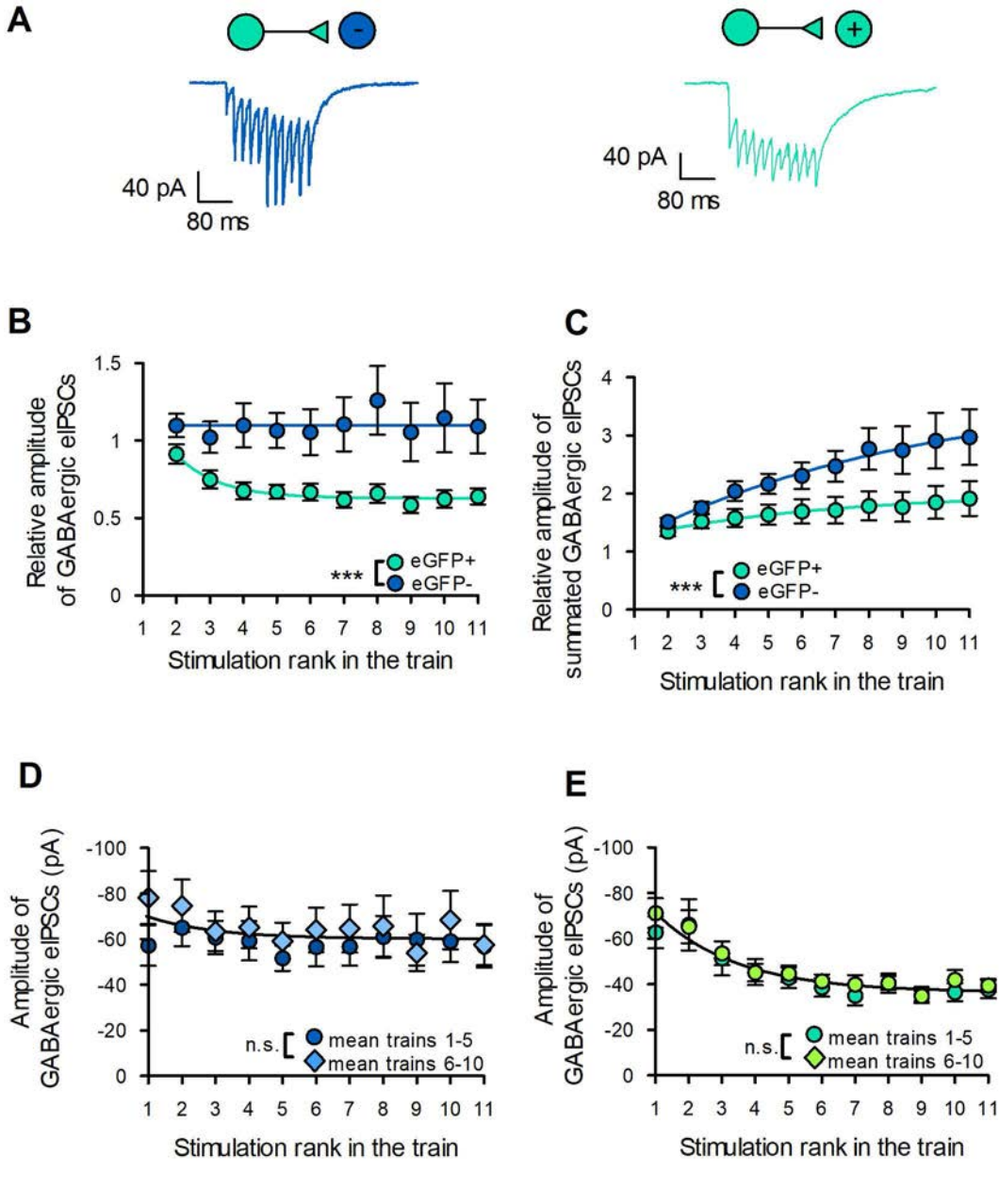
A
40 pA
80 ms
40 pA
80 ms
B
Relative amplitude of GABAergic eIPSCs
1.5
1
0.5
0
***
eGFP+
eGFP-
1 2 3 4 5 6 7 8 9 10 11
Stimulation rank in the train
C
Relative amplitude of summated GABAergic eIPSCs
4
3
2
1
0
***
eGFP+
eGFP-
1 2 3 4 5 6 7 8 9 10 11
Stimulation rank in the train
D
Amplitude of GABAergic eIPSCs (pA)
-100
-80
-60
-40
-20
0
n.s.
mean trains 1-5
mean trains 6-10
1 2 3 4 5 6 7 8 9 10 11
Stimulation rank in the train
E
Amplitude of GABAergic eIPSCs (pA)
-100
-80
-60
-40
-20
0
n.s.
mean trains 1-5
mean trains 6-10
1 2 3 4 5 6 7 8 9 10 11
Stimulation rank in the train

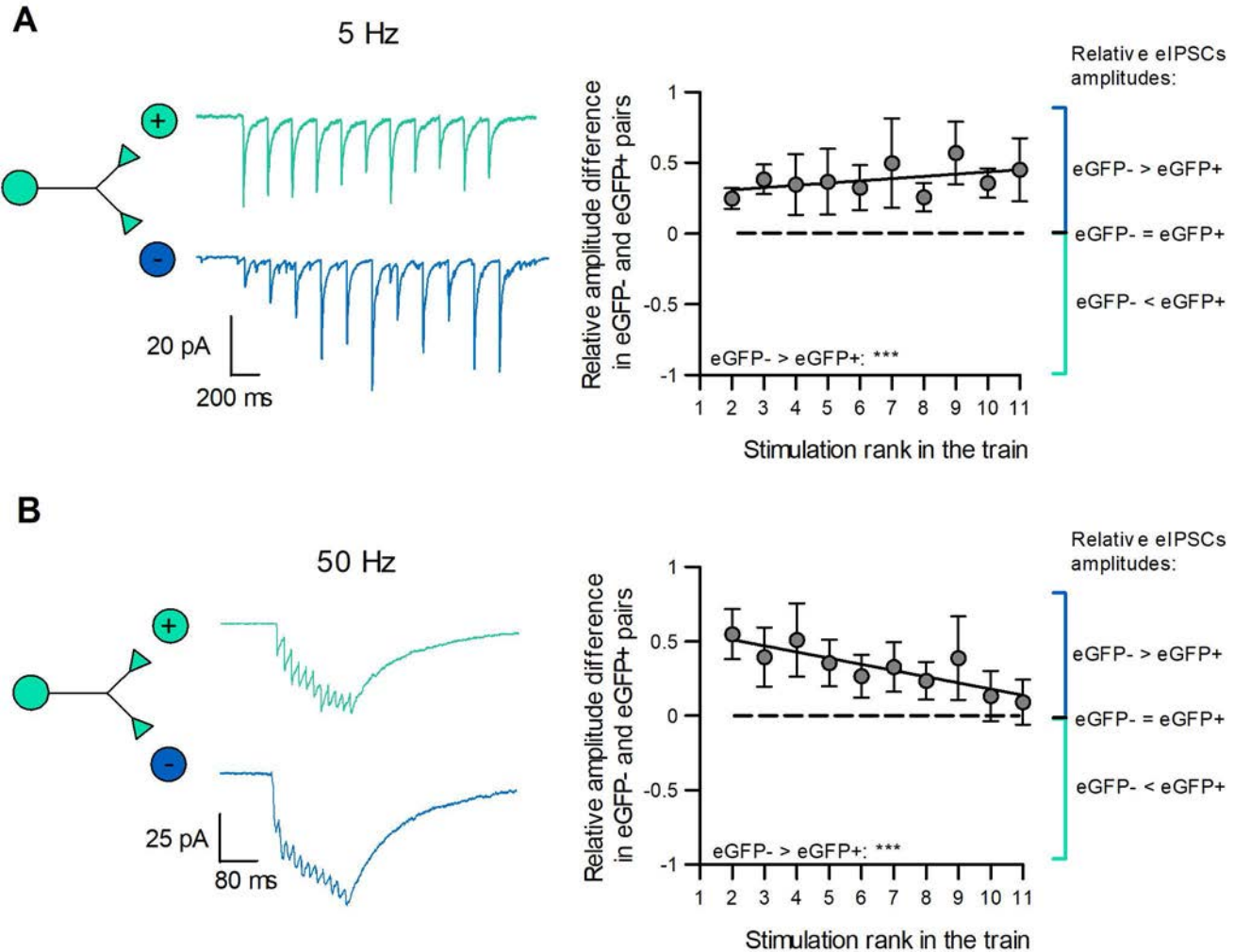
A
5 Hz
+
-
20 pA
200 ms
Relative amplitude difference in eGFP- and eGFP+ pairs
1
0.5
0
-0.5
-1
eGFP- > eGFP+: ***
1 2 3 4 5 6 7 8 9 10 11
Stimulation rank in the train
Relative eIPSCs amplitudes:
eGFP- > eGFP+
eGFP- = eGFP+
eGFP- < eGFP+
B
50 Hz
+
-
25 pA
80 ms
Relative amplitude difference in eGFP- and eGFP+ pairs
1
0.5
0
-0.5
-1
eGFP- > eGFP+: ***
1 2 3 4 5 6 7 8 9 10 11
Stimulation rank in the train
Relative eIPSCs amplitudes:
eGFP- > eGFP+
eGFP- = eGFP+
eGFP- < eGFP+

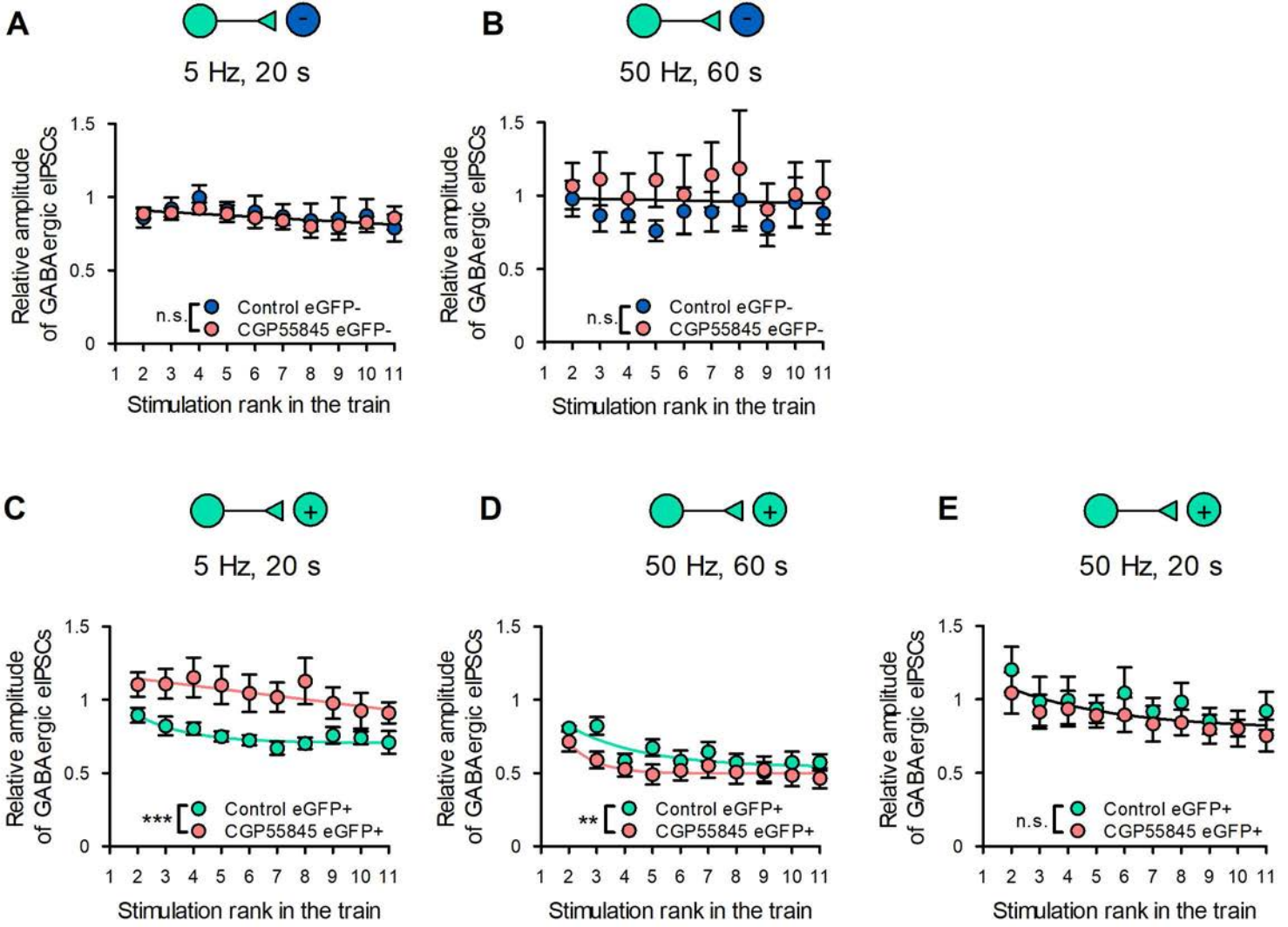
A
5 Hz, 20 s
B
50 Hz, 60 s
Relative amplitude of GABAergic eIPSCs
Stimulation rank in the train
n.s.
Control eGFP-
CGP55845 eGFP-
C
5 Hz, 20 s
D
50 Hz, 60 s
E
50 Hz, 20 s
***
**
Control eGFP+
CGP55845 eGFP+

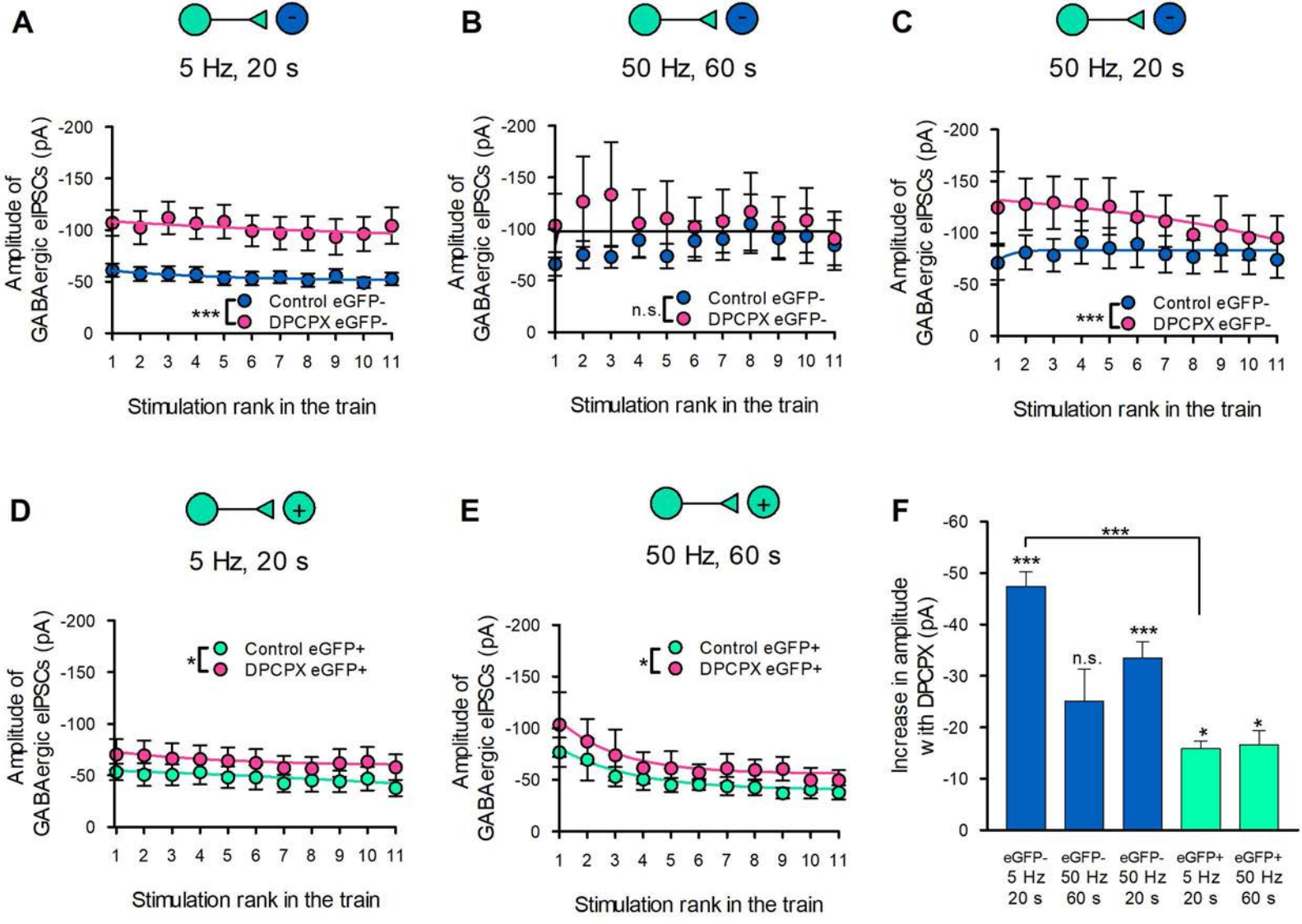
A
5 Hz, 20 s
Amplitude of GABAergic eIPSCs (pA)
-200
-150
-100
-50
0
***
Control eGFP-
DPCPX eGFP-
1 2 3 4 5 6 7 8 9 10 11
Stimulation rank in the train
B
50 Hz, 60 s
Amplitude of GABAergic eIPSCs (pA)
n.s.
Control eGFP-
DPCPX eGFP-
Stimulation rank in the train
C
50 Hz, 20 s
Amplitude of GABAergic eIPSCs (pA)
***
Control eGFP-
DPCPX eGFP-
Stimulation rank in the train
D
5 Hz, 20 s
Amplitude of GABAergic eIPSCs (pA)
*
Control eGFP+
DPCPX eGFP+
Stimulation rank in the train
E
50 Hz, 60 s
Amplitude of GABAergic eIPSCs (pA)
*
Control eGFP+
DPCPX eGFP+
Stimulation rank in the train
F
Increase in amplitude with DPCPX (pA)
-60
-50
-40
-30
-20
-10
0
***
***
n.s.
***
*
*
eGFP- 5 Hz 20 s
eGFP- 50 Hz 60 s
eGFP- 50 Hz 20 s
eGFP+ 5 Hz 20 s
eGFP+ 50 Hz 60 s

Data quantification and analysis

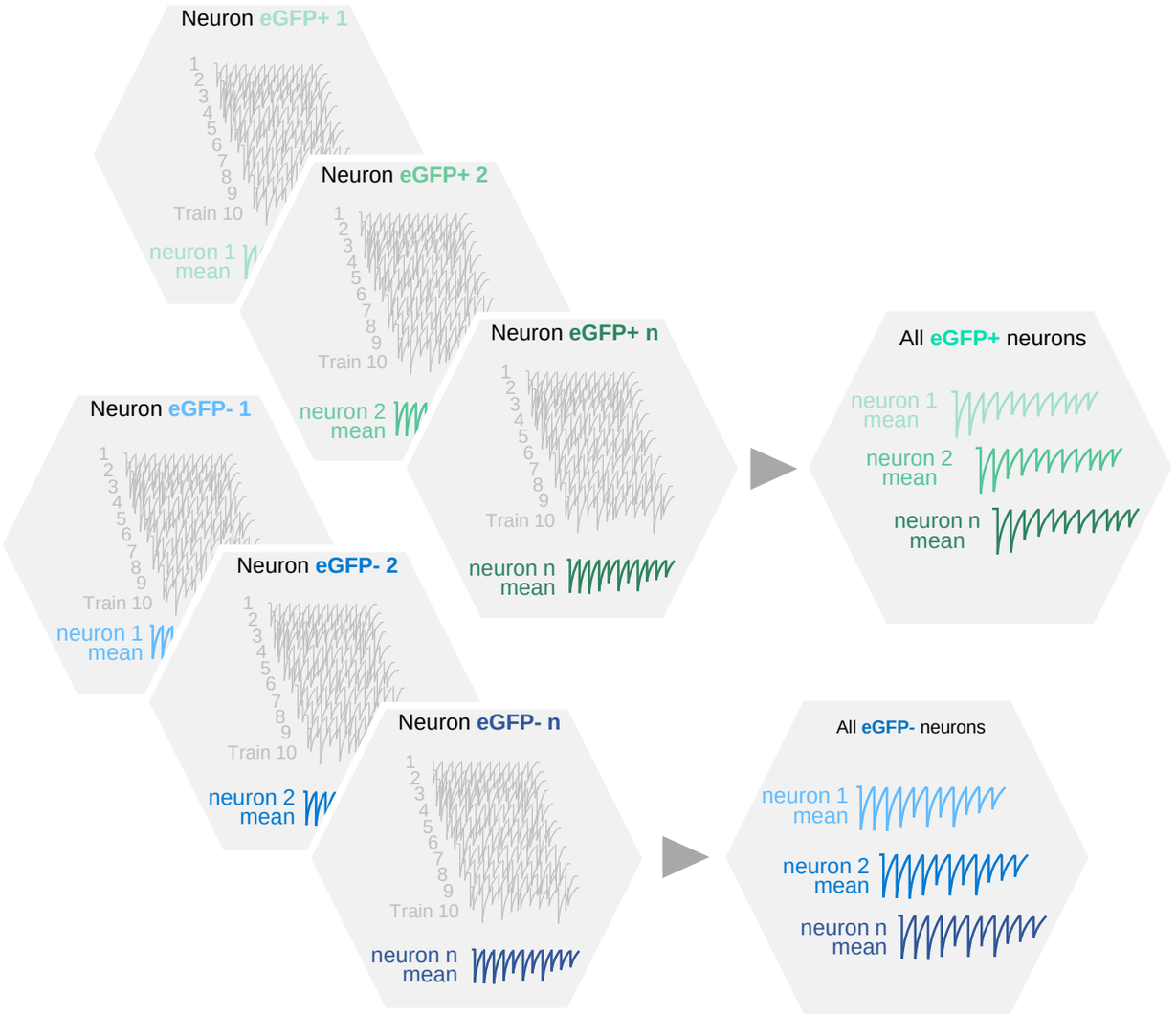

Curve fitting and model comparison

Groups similar or statistically different?

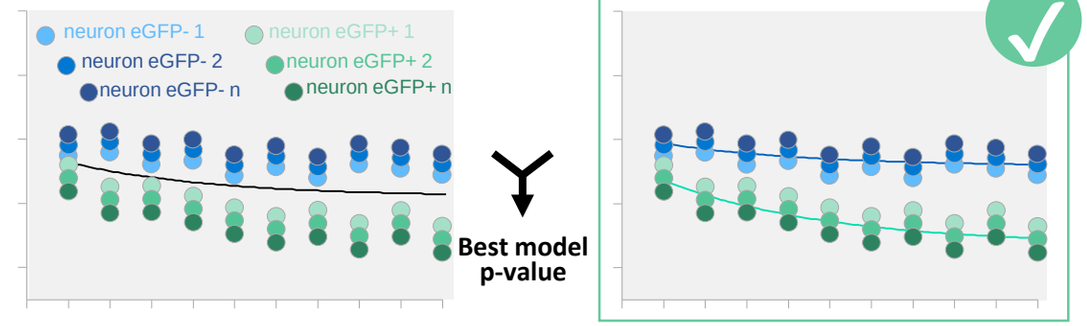

Fit of pooled data with « Equation 3 »

Fit of each group with « Equation 3 »

Plasticity or no plasticity during the train?

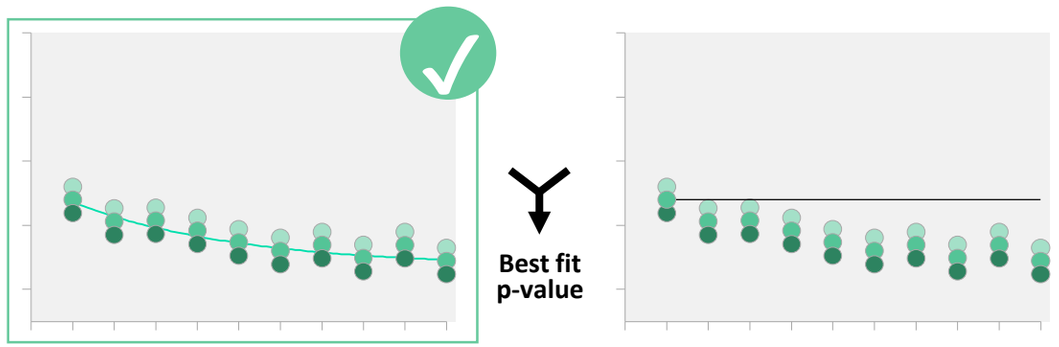

Fit of group data with « Equation 3 »

Linear fit of group data with slope = 0

Illustrations: Curve fits superimposed with average amplitudes

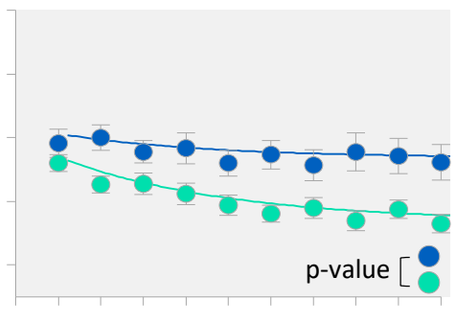

p-value of model comparisons are symbolized in the figures and given in the text. Other criteria of model/fit goodness (BIC, AIC, AICc) are given in the supplementary tables.

Supplementary figure S1. Data quantification, analysis and statistics.

Stimulation protocols were applied ten times in each neuron and the within-cell average across trials was calculated by averaging eIPSCs amplitudes from these ten repetitions. These within-cell average across ten trials were used for statistical analysis. Non-linear regression analysis was used to analyze changes in eIPSCs amplitudes during stimulation train protocols. To compare two different conditions (e.g. eGFP- vs. eGFP+ or presence/absence of antagonists) data from each conditions were fitted with Equation 3, either individually (sum of two functions) or pooled (one single function). When the sum of two individual fits provided statistically significant improvements with respect to the fit of pooled data, the two conditions were considered as having distinct effects. To define whether STP was expressed during trains of stimulations, i.e. whether significant changes in amplitude occurred during the train, fits with Equation 3 were compared with linear fits with slope values forced to 0. When fits with Equation 3 provided statistically significant improvements with respect to the linear fit with slope value forced to 0, the connections were considered as displaying a significant STP during the corresponding protocol. Details of all models (number of neurons, degree of freedom, Residual sum of squares, AIC, AICc, BIC) as well as details of model comparison (F, P, differences in AIC, AICc and BIC) are given in Supplementary table 1. Individual data of all neurons were always used for curve fitting and average values were used for illustration.

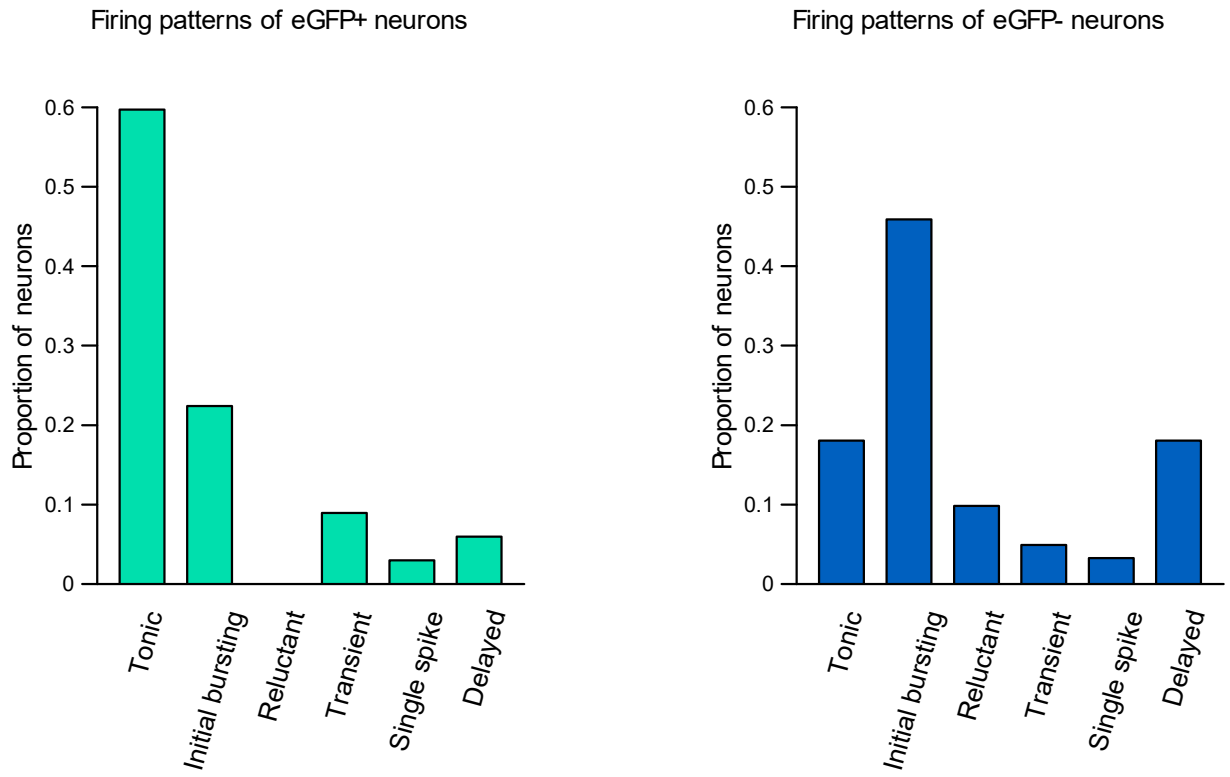

Supplementary figure S2.
Action-potential firing patterns in eGFP+ (left) and eGFP- (right) neurons.
A majority of eGFP+ neurons were of tonic-firing type (Tonic) whereas a majority of eGFP- neurons were of initial bursting type (n = 67 eGFP+ neurons and 61 eGFP- neurons).

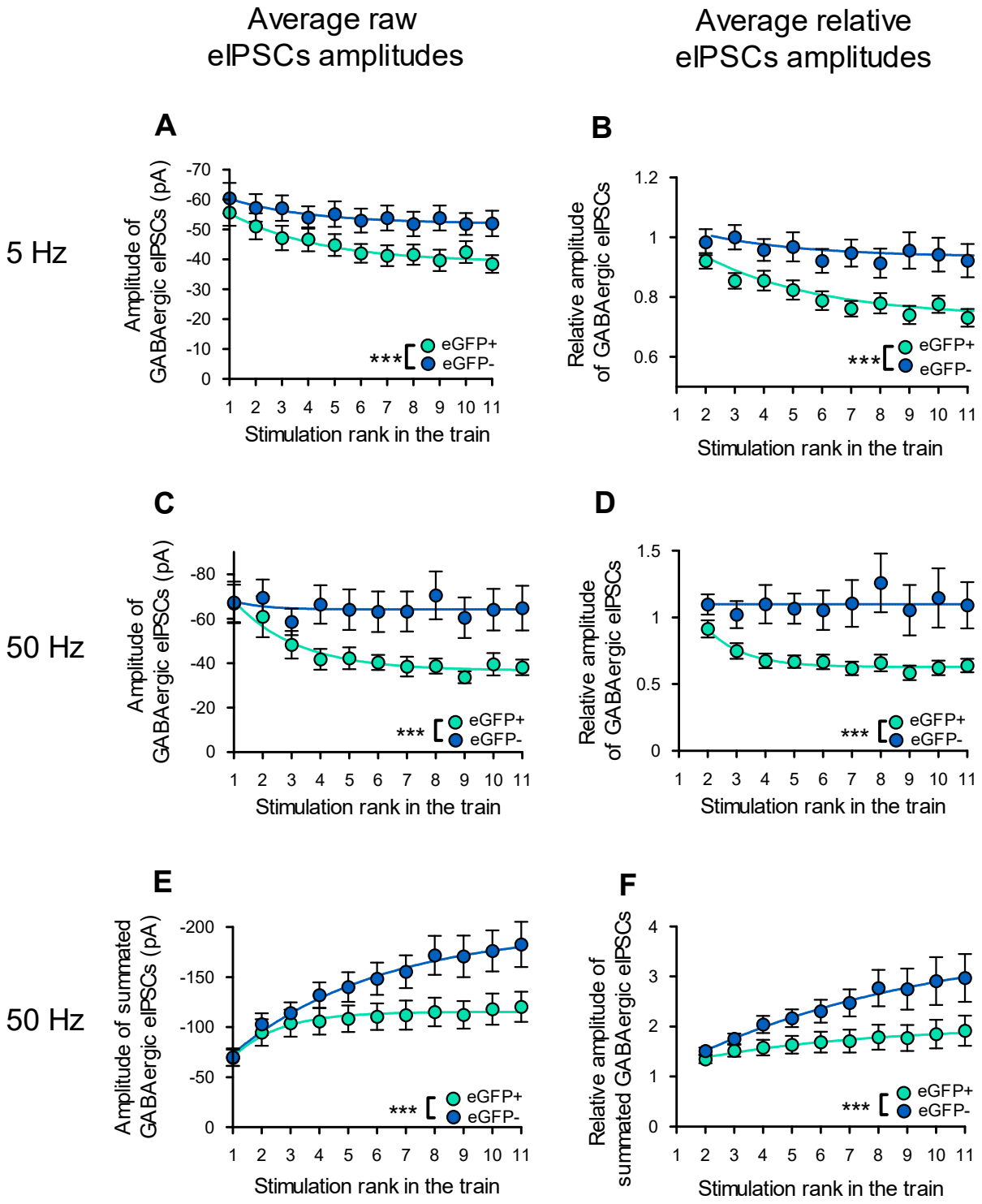

Supplementary figure S3.
Short-term plasticity of GABAergic connections during trains at 5 Hz and 50 Hz.

A. Average raw eIPSCs amplitudes of GABAergic eIPSCs recorded in eGFP- neurons (blue) and eGFP+ neurons (green) during 5 Hz protocols. B. Relative amplitudes of GABAergic eIPSCs recorded in eGFP- and eGFP+ neurons (amplitudes normalized after eIPSCs of rank 1, same neurons as in A). C. Average raw eIPSCs amplitudes of GABAergic eIPSCs recorded in eGFP- neurons (blue) and eGFP+ neurons (green) during 50 Hz protocols. D. Relative amplitudes of GABAergic eIPSCs recorded in eGFP- and eGFP+ neurons (amplitudes normalized after eIPSCs of rank 1, same neurons as in C). E. F. Same data as in C-D, but with eIPSCs measured from the basal current level before the first eIPSC (summated eIPSCs amplitudes). Results of non-linear regressions used to compare conditions are given as P > 0.5: n.s. and P < 0.001: ***. Details of regressions and the corresponding analysis are given in Supplementary Table 1. For 5 Hz protocols: n = 54 eGFP- and n = 49 eGFP+ neurons. For 50 Hz protocols: n = 27 eGFP- and n = 19 eGFP+ neurons.

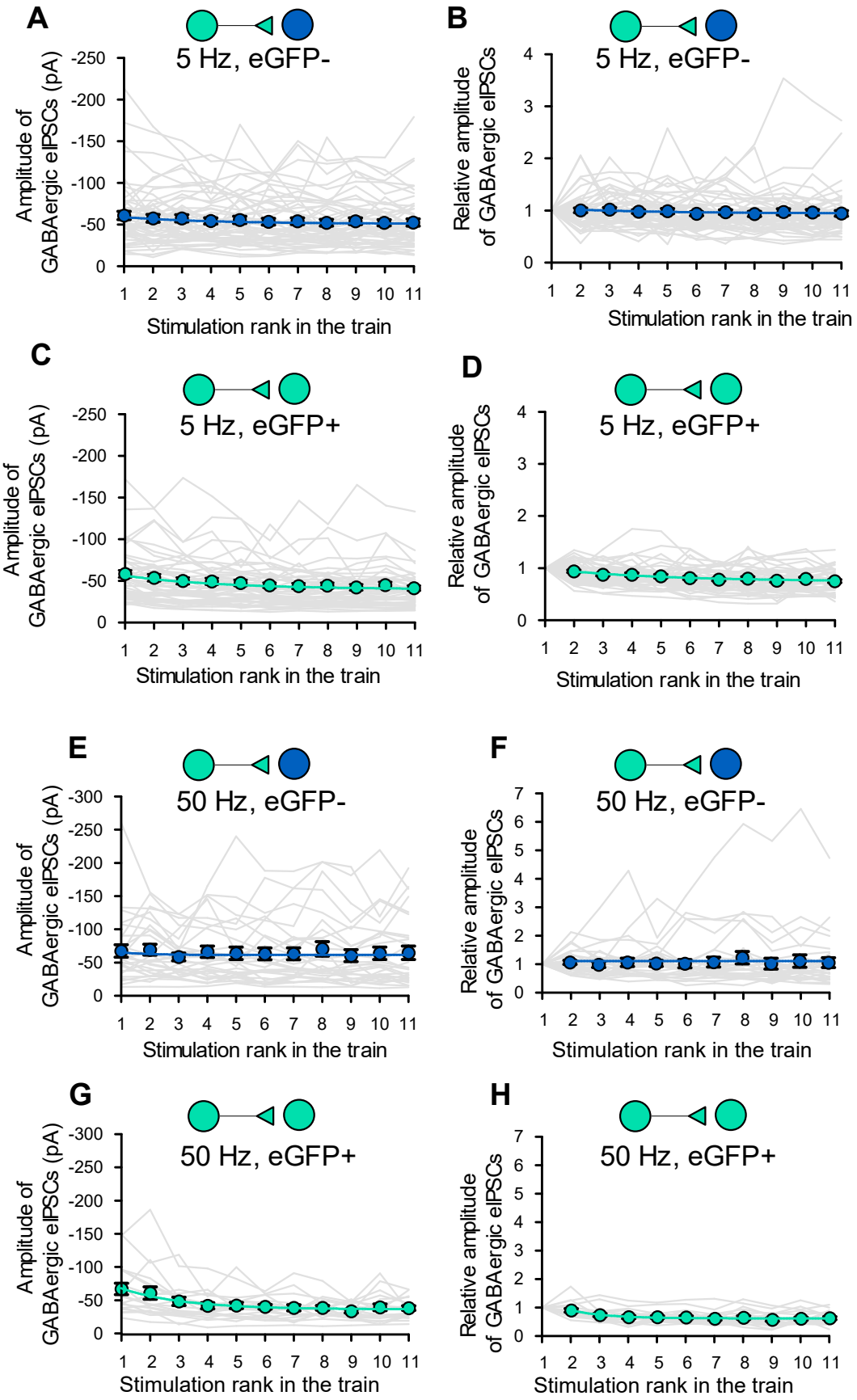

Supplementary figure S4.
Short-term plasticity of GABAergic connections during trains at 5 Hz and 50 Hz: individual neurons.

Left: Average raw eIPSCs amplitudes of GABAergic eIPSCs. Right: Relative amplitudes of GABAergic eIPSCs (amplitudes normalized after eIPSCs of rank 1, same neurons as left).
A-D: train of stimulations at 5 Hz. Same data as in Fig. 3. n = 54 eGFP- and n = 49 eGFP+ neurons. E-H: trains of stimulations at 50 Hz. Same data as in Fig. 4. n = 27 eGFP- and n = 19 eGFP+ neurons.
A, B, E, F: eIPSCs recorded in eGFP- neurons. C, D, G, H: eIPSCs recorded in eGFP+ neurons. Average amplitudes from individual neurons are in grey.

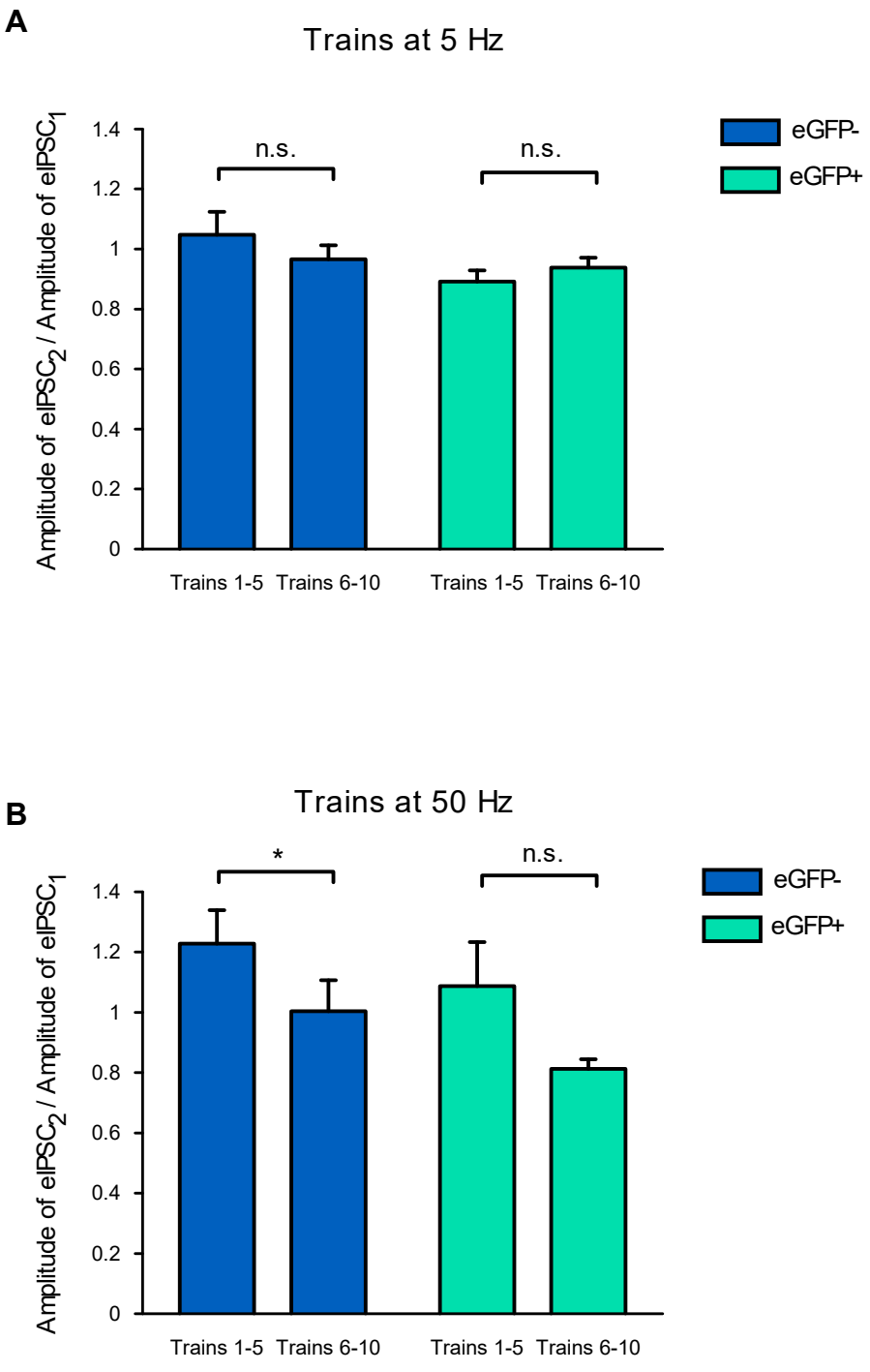

Supplementary figure S5.

Relative amplitude of rank 2 eIPSCs in the first five and the last five trains. A. During 5 Hz trains, eIPSC2/eIPSC1 remained similar in the first five and the last five trains for connections on both eGFP- and eGFP+ neurons (PeGFP- = 0.678, PeGFP+ = 0.223, Wilcoxon Signed Rank Test for Paired Data). B. During 50 Hz trains, eIPSC2/eIPSC1 remained similar in the first five and the last five trains for connections on eGFP+ neurons (PeGFP+ = 0.098, Wilcoxon Signed Rank Test for Paired Data), but significantly decreased by 18% for eGFP- neurons (PeGFP- = 0.048, Wilcoxon Signed Rank Test for Paired Data). This suggests that the facilitation observed in eGFP- neurons during paired-pulse stimulation at short intervals (Fig. 2E) is replaced by other types of plasticities during repeated trains of stimulation at 50 Hz.

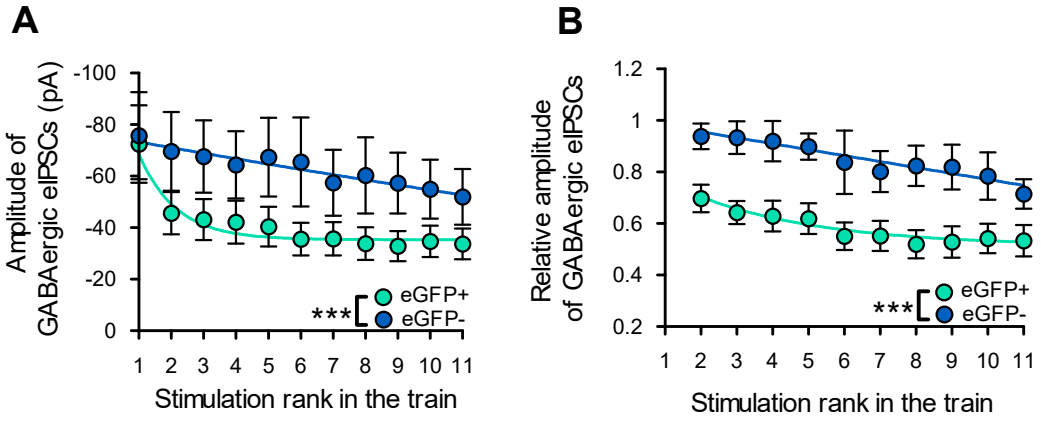

Supplementary figure S6.
Short-term plasticity of GABAergic connections during trains of stimulations at 5 Hz with increased amplitudes of stimulation.
For this experiment, stimulation amplitudes were set at 0.45 mA (versus 0.21 mA on average for all other experiments). A. Average raw eIPSCs amplitudes of GABAergic eIPSCs recorded in eGFP- neurons (blue) and eGFP+ neurons (green). B. Relative amplitudes of GABAergic eIPSCs recorded in eGFP- and eGFP+ neurons (amplitudes normalized after eIPSCs of rank 1, same neurons as in A). n = 11 eGFP- and n = 11 eGFP+ neurons.
Evolution of eIPSCs amplitudes during the trains were significantly different in eGFP- and eGFP+ neurons as it was observed with lower amplitudes of stimulation (Fig. 3). This indicated that changes in stimulation efficacy during trains of stimulations were unlikely to influence our results.

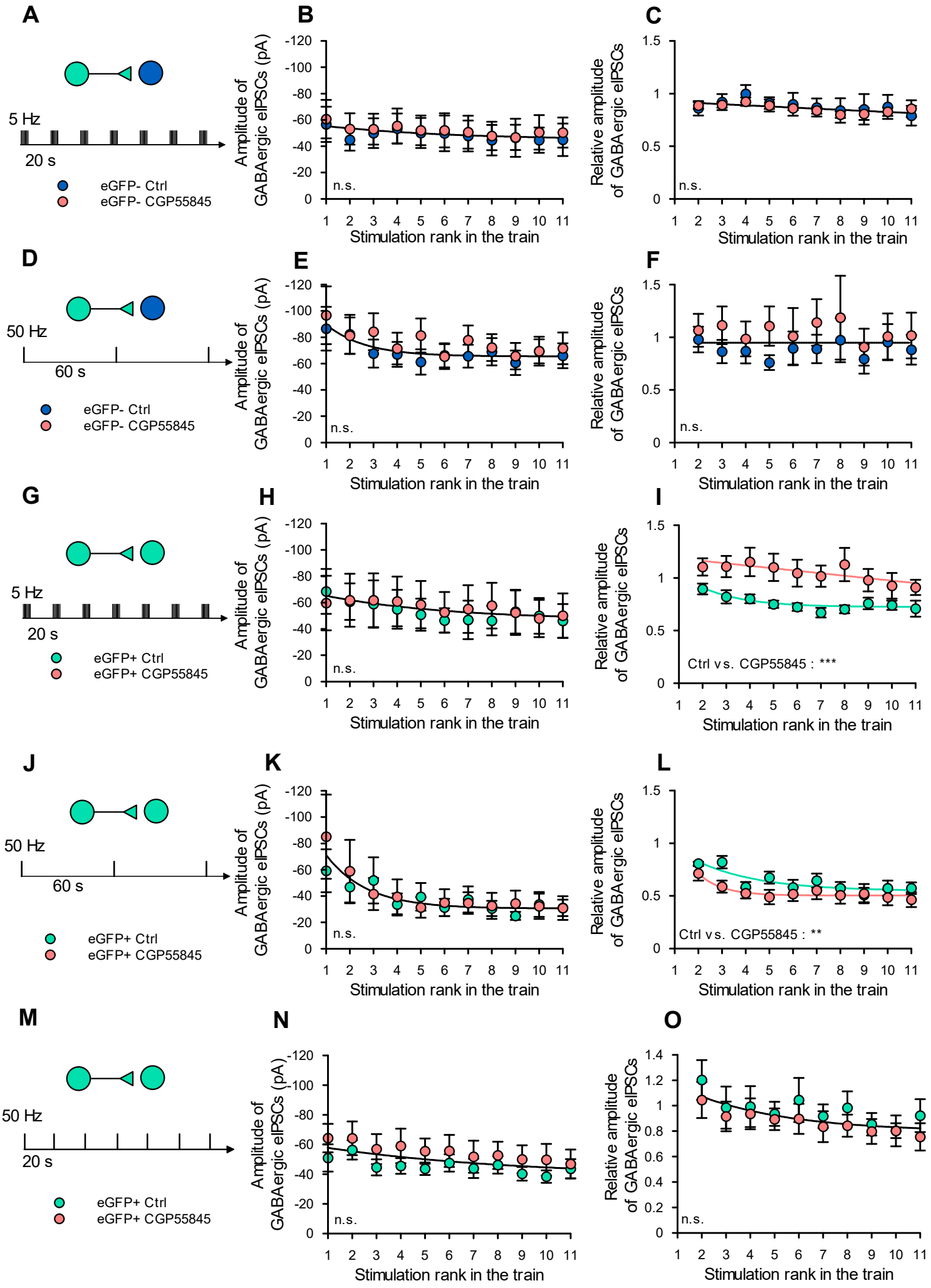

Supplementary figure S7.
Effect of a $GABA_B$ receptor antagonist on GABAergic eIPSCs during 5 Hz and 50 Hz trains.
legend next page

Supplementary figure S7.
Effect of a $GABA_B$ receptor antagonist on GABAergic eIPSCs during 5 Hz and 50 Hz trains.

Average amplitudes of GABAergic eIPSCs during trains at 5 Hz and 50 Hz before (blue and green) and during bath application of 10 µM CGP55845 (orange), a $GABA_B$ receptors antagonist. For each neuron, trains of 11 stimulations were repeated 10 times in control condition and 10 times during bath application of CGP55845. A, D, G, J, M. Type of neuron (eGFP- or eGFP+), frequency of stimulation (5 Hz or 50 Hz) and interval between trains (20 s or 60 s) applied in B-C, E-F, H-I, K-L, N-O, respectively. B, E, H, K, N. Average raw eIPSCs amplitudes. C, F, I, L, O. Average relative eIPSCs amplitudes. A-F: CGP55845 had no effect on GABAergic connections onto eGFP- neurons, neither during trains at 5 Hz (A-C, n = 6 neurons) nor during trains at 50 Hz (D-F n = 12 neurons). G-O: in eGFP+ neurons CGP55845 did not changed raw eIPSCs amplitudes (H, K, N), but it significantly increased relative eIPSCs amplitude during 5 Hz trains repeated every 20 s (I, n = 8 neurons), indicating a phasic inhibition involving GABAB receptors during these trains. Evolution of eIPSCs amplitudes during trains were compared with non-linear regression. Details of regressions and the corresponding analysis are given in Supplementary Table 7. $P > 0.5$: n.s. and $P < 0.001$: ***.

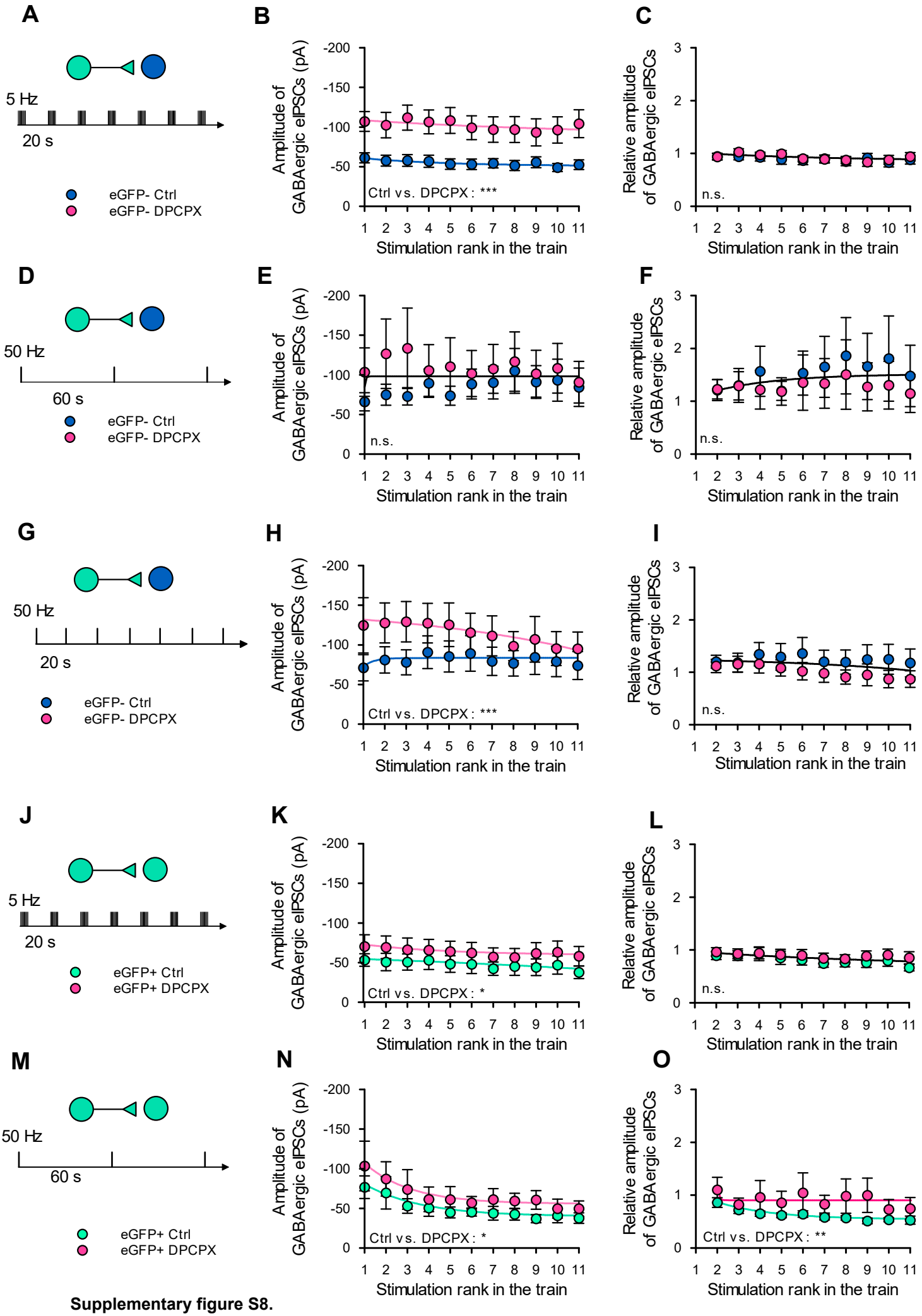

Supplementary figure S8.
Effect of an A1 adenosine receptor antagonist on GABAergic eIPSCs during 5 Hz and 50 Hz trains.
legend next page

Supplementary figure S8.
Effect of an A1 adenosine receptor antagonist on GABAergic eIPSCs during 5 Hz and 50 Hz trains.
legend next page

Average amplitudes of GABAergic eIPSCs during trains at 5 Hz and 50 Hz before (blue and green) and during bath application of 10 µM DPCPX (pink), an A1 receptor antagonist. For each neuron, trains of 11 stimulations were repeated 10 times in control condition and 10 times during bath application of DPCPX. A, D, G, J, M. Type of neuron (eGFP- or eGFP+), frequency of stimulation (5 Hz or 50 Hz) and interval between trains (20 s or 60 s) applied in B-C, E-F, H-I, K-L, N-O, respectively. B, E, H, K, N. Average raw eIPSCs amplitudes. C, F, I, L, O. Average relative eIPSCs amplitudes. B, H. DPCPX significantly increased raw eIPSCs amplitudes recorded in eGFP- neurons during trains at 5 Hz repeated every 20 s (B, n = 9 neurons) and 50 Hz repeated every 20 s (H, n = 9 neurons) but had no effect on raw eIPSCs amplitudes recorded during trains at 50 Hz repeated every 60 s (E, n = 7 neurons). This indicated a tonic inhibition of GABAergic connections onto eGFP- neurons by adenosine depending on the delay between trains of stimulation. K, N, in eGFP+ neurons, DPCPX significantly increased raw eIPSCs amplitudes during 5 Hz trains repeated every 20 s (K) and 50 Hz trains repeated every 60 s (N). This indicated a tonic inhibition of GABAergic connections onto eGFP+ neurons. C, F, I, L, O Except during 50 Hz trains repeated every 60 s where a weak significant effect was recorded (O), no effect of DPCPX was detected in relative eIPSCs amplitudes, neither in eGFP- nor in eGFP+ neurons indicating that inhibition involving A1 receptors did not changed during the train. Evolution of eIPSCs amplitudes during trains were compared with non-linear regression. Details of regressions and the corresponding analysis are given in Supplementary Table 8. $P > 0.5$: n.s., $0.05 > P > 0.01$: *, $P < 0.001$: ***.

Supplementary Table 1. Non linear regressions FIGURE 2

Stimulation protocol						Model parameters determined by non linear curve fitting														Model comparison stats		
Figure	Paired-Pulse ISI: 20, 50, 75, 100, 200, 300 ms	Type of data	eGFP condition	Drug condition	Model	N neurons	N obs	k	A1 eGFP-	A2 eGFP-	A3 eGFP-	A1 eGFP+	A2 eGFP+	A3 eGFP+	SS	df	AIC	AICc	BIC	F	p	dAICc
2E		PPR	- and +	Control	"equation 2" pooled data	63-	223	3	1.29	1.01	34.04	1.29	1.01	34.04	25.41	220	156.48	164.67	170.11			
					sum of two "equation 2"	52+	223	6	1.53	1.07	28.46	1.06	0.95	68.52	24.04	217	150.12	164.65	173.97	4.1222	**7.20E-03**	**0.02**

Supplementary Table 2. Non linear regressions FIGURE 3

Stimulation protocol								Model parameters determined by non linear curve fitting														Model comparison stats		
Figure	Freqency	protocol interval	Protocol repetition	Type of data	eGFP condition	Drug condition	Model	N neurons	N obs	k	A1 eGFP-	A2 eGFP-	A3 eGFP-	A1 eGFP+	A2 eGFP+	A3 eGFP+	SS	df	AIC	AICc	BIC	F	p	dAICc
S3A	5 Hz	20 s	1-10	Raw	- and +	Control	sum of two exponential fits, same intercept A1	54-	1133	5	-58.06	7.80	6.46	-58.06	18.23	2.56	928309.68	1128	10828.04	10840.12	10858.24			
							sum of two "Equation3"	49+	1133	6	-60.20	8.32	3.12	-55.42	16.42	3.38	927586.17	1127	10829.16	10843.26	10864.39	0.8791	3.49E-01	-3.14
S3A	5 Hz	20 s	1-10	Raw	- and +	Control	"Equation3" pooled data	54-	1133	3	-57.93	12.17	3.29	-57.93	12.17	3.29	957197.83	1130	10858.76	10866.80	10878.89			
							sum of two "Equation3"	49+	1133	6	-60.20	8.32	3.12	-55.42	16.42	3.38	927586.17	1127	10829.16	10843.26	10864.39	11.9925	**9.88E-08**	**23.54**
S3A	5 Hz	20 s	1-10	Raw	-	Control	Linear fit slope=0	54-	594	1	-54.56	0.00					573961.45	593	5772.52	5776.54	5781.30			
							Exponential (Equation3)		594	3	-60.20	8.32	3.12				570329.12	591	5772.75	5780.82	5790.30	1.8820	1.53E-01	-4.28
S3A	5 Hz	20 s	1-10	Raw	+	Control	Linear fit slope=0	49+	539	1				-44.60	0.00		369871.83	538	5053.93	5057.95	5062.51			
							Exponential (Equation3)		539	3				-55.42	16.42	3.38	357257.05	536	5039.23	5047.30	5056.39	9.4631	**9.14E-05**	**10.65**
3B, S3B	5 Hz	20 s	1-10	Norm	- and +	Control	"Equation3" pooled data	54-	1030	3	0.96	-0.13	3.79	0.96	-0.13	3.79	93.83	1027	463.28	471.32	483.03			
							sum of two "Equation3"	49+	1030	6	0.99	-0.07	3.48	0.92	-0.19	3.99	87.89	1024	401.99	416.10	436.56	23.0422	**1.94E-14**	**55.21**
3B, S3B	5 Hz	20 s	1-10	Norm	-	Control	Linear fit slope=0	54-	540	1	0.95	0.00					66.92	539	408.87	412.89	417.45			
							Exponential (Equation3)		540	3	0.99	-0.07	3.48				66.72	537	411.27	419.34	428.44	0.7974	4.51E-01	-6.451
3B, S3B	5 Hz	20 s	1-10	Norm	+	Control	Linear fit slope=0	49+	490	1				0.80	0.00		22.66	489	-111.61	-107.59	-103.22			
							Exponential (Equation3)		490	3				0.92	-0.19	3.99	21.33	487	-137.19	-129.11	-120.42	15.1532	**4.13E-07**	**21.52**
3C	5 Hz	20 s	1-10 1-5 6-10	Raw	-	Control	"Equation3" pooled data	50-	1100	3	-61.52	9.25	2.74	-61.52	9.25	2.74	1141933.80	1097	10769.35	10777.39	10789.36			
							sum of two "Equation3"		1100	6	-63.28	10.39	1.65	-59.81	12.94	9.61	1141274.39	1094	10774.71	10788.82	10809.74	0.2107	8.89E-01	-11.43
3D	5 Hz	20 s	1-10 1-5 6-10	Raw	+	Control	"Equation3" pooled data	43+	946	3	-55.61	15.11	3.31	-55.61	15.11	3.31	748490.65	943	9005.83	9013.87	9025.24			
							sum of two "Equation3"		946	6	-54.05	16.14	3.78	-57.19	14.23	2.89	745656.50	940	9008.24	9022.36	9042.21	1.1909	3.12E-01	-8.49

Supplementary Table 3. Supplementary Figure 6 Non linear regressions stimulation at 5Hz at increased stimulation amplitude

Stimulation protocol							Model parameters determined by non linear curve fitting														Model comparison stats		
Figure	Freqency	protocol interval	Protocol repetition	Type of data	eGFP condition	Drug condition	Model	N neurons	N obs	k	A1 eGFP-	A2 eGFP-	A3 eGFP-	A1 eGFP+	A2 eGFP+	A3 eGFP+	SS	df	AIC	AICc	BIC	F	p	dAICc
S6A	5 Hz	20 s	1-10	Raw	- and +	Control	"Equation3" pooled data	11-	242	3	-71.30	26.74	2.53	-71.30	26.74	2.53	351728.28	239	2456.93	2465.10	2470.89			
							sum of two "Equation3"	11+	242	6	-71.22	35.90	1.14	-73.38	160.72	73.12	319721.69	236	2439.84	2454.32	2464.27	7.8751	**4.98E-05**	**10.78**
S6B	5 Hz	20 s	1-10	Norm	- and +	Control	"Equation3" pooled data	11-	220	3	0.82	-0.29	8.59	0.82	-0.29	8.59	14.31	217	31.21	39.40	44.78			
							sum of two "Equation3"	11+	220	6	0.95	-114.51	4954.04	0.70	-0.19	3.58	10.40	214	-33.11	-18.58	-9.35	26.8655	**8.70E-15**	**57.98**

Supplementary Table 4. Non linear regressions FIGURE 4

Stimulation protocol							Model parameters determined by non linear curve fitting														Model comparison stats			
Figure	Freqency	protocol interval	Protocol repetitio	Type of data	eGFP condition	Drug condition	Model	N neurons	N obs	k	A1 eGFP-	A2 eGFP-	A3 eGFP-	A1 eGFP+	A2 eGFP+	A3 eGFP+	SS	df	AIC	AICc	BIC	F	p	dAICc
S3C	50 Hz	60 s	1-10	Raw	- and +	Control	"Equation3" pooled data	27-	517	3	-68.28	14.98	1.82	-68.28	14.98	1.82	855892.23	514	5307.11	5315.19	5324.10			
							sum of two "Equation3"	19+	517	6	-68.03	3.88	1.01	-68.49	31.86	2.18	795499.75	511	5275.28	5289.50	5305.02	12.9313	**3.73E-08**	**25.69**
S3C	50 Hz	60 s	1-10	Raw	-	Control	Linear fit slope=0	27-	308	1	-64.71	0.00					682823.28	307	3250.86	3254.90	3258.32			
							Exponential (Equation3)		308	3	-68.03	3.88	1.01				682430.74	305	3254.69	3262.82	3269.61	0.0877	9.16E-01	-7.92
S3C	50 Hz	60 s	1-10	Raw	+	Control	Linear fit slope=0	19+	209	1				-44.45	0.00		132402.80	208	1945.43	1949.49	1952.12			
							Exponential (Equation3)		209	3				-68.49	31.86	2.18	113069.01	206	1916.44	1924.64	1929.81	17.6121	**8.69E-08**	**24.85**
4B, S3D	50 Hz	60 s	1-10	Norm	- and +	Control	"Equation3" pooled data	27-	470	3	1.02	-0.10	0.07	1.02	-0.10	0.07	233.23	467	1012.46	1020.55	1029.08			
							sum of two "Equation3"	19+	470	6	1.10	0.10	8.17	0.91	-0.28	1.26	212.36	464	974.40	988.64	1003.47	15.2018	**1.88E-09**	**31.91**
4B, S3D	50 Hz	60 s	1-10	Norm	-	Control	Linear fit slope=0	27-	280	1	1.10	0.00					201.79	279	706.89	710.93	714.16			
							Exponential (Equation3)		280	3	1.10	0.10	8.17				201.65	277	710.69	718.84	725.23	0.0956	9.09E-01	-7.909
4B, S3D	50 Hz	60 s	1-10	Norm	+	Control	Linear fit slope=0	19+	190	1				0.68			11.96	189	17.83	21.89	24.32			
							Exponential (Equation3)		190	3				0.91	-0.28	1.26	10.57	187	-1.77	6.45	11.22	12.3666	**9.03E-06**	**15.45**
S3E	50 Hz	60 s	1-10	Raw Summ.	- and +	Control	"Equation3" pooled data	27-	506	3	-74.18	-86.24	3.95	-74.18	-86.24	3.95	2907009.78	503	5823.95	5832.03	5840.86			
							sum of two "Equation3"	19+	506	6	-74.27	-123.33	5.07	-71.05	-44.47	1.60	2698637.74	500	5792.32	5806.54	5821.90	12.8690	**4.12E-08**	**25.49**
S3E	50 Hz	60 s	1-10	Raw Summ.	-	Control	Linear fit slope=0	27-	297	1	-142.14	0.00					2405477.14	296	3519.71	3523.75	3527.10			
							Exponential (Equation3)		297	3	-74.27	-123.33	5.07				2076127.99	294	3479.98	3488.11	3494.75	23.3195	**3.98E-10**	**35.64**
S3E	50 Hz	60 s	1-10	Raw Summ.	+	Control	Linear fit slope=0	19+	209	1				-106.84	0.00		659375.99	208	2280.97	2285.03	2287.65			
							Exponential (Equation3)		209	3				-71.05	-44.47	1.60	622509.74	206	2272.94	2281.14	2286.31	6.0999	**2.67E-03**	**3.89**
4C, S3F	50 Hz	60 s	1-10	rm Sum	- and +	Control	"Equation3" pooled data	27-	450	3	1.46	1.62	8.17	1.46	1.62	8.17	876.68	457	1585.15	1593.24	1601.59			
							sum of two "Equation3"	19+	450	6	1.51	2.29	8.70	1.38	0.64	6.06	815.54	454	1558.62	1572.87	1587.38	11.0962	**4.90E-07**	**20.37**
4C, S3F	50 Hz	60 s	1-10	rm Sum	-	Control	Linear fit slope=0	27-	270	1	2.36	0.00					731.22	269	1039.23	1043.27	1046.42			
							Exponential (Equation3)		270	3	1.51	2.29	8.70				671.52	267	1020.23	1028.38	1034.62	11.8691	**1.15E-05**	**14.89**
4C, S3F	50 Hz	60 s	1-10	rm Sum	+	Control	Linear fit slope=0	19+	180	1				1.68	0.00		148.47	189	480.16	484.23	486.54			
							Exponential (Equation3)		180	3				1.38	0.64	6.06	144.02	187	478.68	486.91	491.45	2.7350	6.76E-02	-2.682
4D	50 Hz	60 s	1-10 1-5 6-10	Raw	-	Control	"Equation3" pooled data	22-	484	3	-69.41	9.97	2.04	-69.41	9.97	2.04	943143.46	481	5047.78	5055.86	5064.51			
							sum of two "Equation3"		484	6	-60.37	2.61	2.88	-79.15	17.68	1.65	935579.40	478	5049.88	5064.12	5079.16	1.2882	2.78E-01	-8.25
4E	50 Hz	60 s	1-10 1-5 6-10	Raw	+	Control	"Equation3" pooled data	17+	374	3	-71.91	34.62	2.42	-71.91	34.62	2.42	237187.61	371	3482.55	3490.65	3498.24			
							sum of two "Equation3"		374	6	-67.00	33.18	3.23	-77.60	37.33	1.80	235260.35	368	3485.49	3499.80	3512.96	1.0049	3.91E-01	-9.15

Supplementary Table 5. Non linear regression comparion 5 Hz with 50 Hz FIGURE 3 and 4

Stimulation protocol							Model parameters determined by non linear curve fitting														Model comparison stats			
Figure	Freq ency	interval	num ber	Data type	eGFP	Drug condition	Model	N neurons	N obs	k	A1 5Hz	A2 5Hz	A3 5Hz	A1 50Hz	A2 50Hz	A3 50Hz	SS	df	AIC	AICc	BIC	F	p	dAICc
3B, 4B	5Hz 50Hz	20s 60s	1-10	Norm	-	Control	"Equation3" pooled data	54@5Hz	820	3	1.02	-0.02	0.98	1.02	-0.02	0.98	272.71	817	1432.32	1440.37	1451.16			
							sum of two "Equation3"	27@50H	820	6	0.99	-0.07	3.48	1.10	0.00	0.06	268.48	814	1425.50	1439.63	1458.46	4.2777	**5.23E-03**	**0.738**
3B, 4B	5Hz 50Hz	20s 60s	1-10	Norm	+	Control	"Equation3" pooled data	49@5Hz	680	3	0.91	-0.20	2.52	0.91	-0.20	2.52	34.09	877	-97.54	-89.48	-79.45			
							sum of two "Equation3"	19@50H	680	6	0.92	-0.19	3.99	0.91	-0.28	1.26	31.77	874	-139.40	-125.23	-107.75	16.3811	**2.76E-10**	**35.75**

Supplementary Table 6. Linear regressions FIGURE 5

Stimulation protocol								N						Model comparison stats					
Figure	Freqency	protocol interval	Protocol repetition	Type of data	eGFP condition		Model		N obs	k		SS	df	AIC	AICc	BIC	F	p	dAICc
5A	5 Hz	20 s	1-10	Relativ			y=0x+0	6pairs	10	0		1.99	10	14.25	16.75	14.56			
							y=A1+A2*x		10	2		0.07	8	-15.02	-5.02	-14.11	107.4780	**1.66E-06**	**21.78**
5B	50 Hz	60 s	1-10	Relativ			y=0x+0	4pairs	10	0		1.25	10	9.59	12.09	9.89			
							y=A1+A2*x		10	2		0.05	8	-17.74	-7.74	-16.83	87.7696	**3.61E-06**	**19.83**

Supplementary Table 7. Non linear regressions FIGURE 6 and supplementary figure S7

Stimulation protocol							Model parameters										Model comparison stats								
Figure	Freq.	protocol interval	Protocol repetitio	Type of data	eGFP condition	Drug condition	Model	N neurons	N obs	k	A1 control	A2 control	A3 control	A1 CGP55845	A2 CGP55845	A3 CGP55845	SS	df	AIC	AICc	BIC	F	p	dAICc
S7B	5 Hz	20 s	1-10	Raw	-	Control &	"Equation3" pooled data	6	132	3	-55.81	10.62	5.56	-55.81	10.62	5.56	96495.70	129	1253.07	1261.38	1264.60			
						CGP55845	sum of two "Equation3"		132	6	-52.61	3459.37	4153.92	-59.07	10.23	2.98	96024.87	126	1258.42	1273.32	1278.60	0.2059	8.92E-01	-11.94
6A, S7C	5 Hz	20 s	1-10	Norm	-	Control &	"Equation3" pooled data	6	120	3	0.92	-1.32	120.00	0.92	-1.32	120.00	3.63	117	-71.40	-63.05	-60.25			
						CGP55845	sum of two "Equation3"		120	6	0.93	-1.75	145.23	0.91	-0.13	8.31	3.61	114	-66.02	-51.02	-46.50	0.1962	8.99E-01	-12.03
S7E	50 Hz	60 s	1-10	Raw	-	Control &	"Equation3" pooled data	12	264	3	-91.97	24.14	1.64	-91.97	24.14	1.64	427700.08	261	2708.22	2716.37	2722.52			
						CGP55845	sum of two "Equation3"		264	6	-88.18	23.18	1.42	-95.27	25.24	2.12	424394.75	258	2712.17	2726.61	2737.20	0.6698	5.71E-01	-10.23
6B, S7F	50 Hz	60 s	1-10	Norm	-	Control &	"Equation3" pooled data	12	240	3	1.02	-0.06	0.04				98.52	237	475.41	483.58	489.33			
						CGP55845	sum of two "Equation3"		240	6	0.97	-0.10	0.06	1.09	-0.12	12.47	96.74	234	477.02	491.51	501.39	1.4381	2.32E-01	-7.928
S7H	5 Hz	20 s	1-10	Raw	+	Control &	"Equation3" pooled data	8	176	3	-64.68	18.77	5.30	-64.68	18.77	5.30	326569.82	173	1832.03	1840.26	1844.71			
						CGP55845	sum of two "Equation3"		176	6	-68.78	21.47	2.39	-61.77	-7.10	-9.55	325296.18	170	1837.34	1852.01	1859.53	0.2219	8.81E-01	-11.74
6C, S7I	5 Hz	20 s	1-10	Norm	+	trol & CGP5	"Equation3" pooled data	8	160	3	1.00	-0.37	13.53				12.67	157	56.28	64.54	68.58			
							sum of two "Equation3"		160	6	0.90	-0.19	1.83	1.15	-85.77	3662.80	9.20	154	11.19	25.92	32.71	19.3142	**1.11E-10**	**38.62**
S7K	50 Hz	60 s	1-10	Raw	+	Control &	"Equation3" pooled data	6	132	3	-71.90	40.46	1.73	-71.90	40.46	1.73	115572.90	129	1276.88	1285.20	1288.41			
						CGP55845	sum of two "Equation3"		132	6	-58.81	30.01	3.00	-85.57	53.08	1.30	113173.57	126	1280.11	1295.01	1300.29	0.8904	4.48E-01	-9.82
6D, S7L	50 Hz	60 s	1-10	Norm	+	Control &	"Equation3" pooled data	6	120	3	0.77	-0.24	1.86				3.12	117	-89.37	-81.02	-78.22			
						CGP55845	sum of two "Equation3"		120	6	0.83	-0.28	2.67	0.72	-0.21	1.00	2.80	114	-96.39	-81.39	-76.88	4.3568	**6.05E-03**	**0.373**
S7N	50 Hz	20 s	1-10	Raw	+	Control &	"Equation3" pooled data	7	154	3	-58.68	19.42	7.85	-58.68	19.42	7.85	69256.72	151	1385.76	1394.03	1397.91			
						CGP55845	sum of two "Equation3"		154	6	-52.86	13.12	5.00	-64.52	30.88	12.81	65781.93	148	1383.83	1398.60	1405.09	2.6059	5.40E-02	-4.57
6E, S7O	50 Hz	20 s	1-10	Norm	+	Control &	"Equation3" pooled data	7	140	3	1.08	-0.28	3.90	1.08	-0.28	3.90	13.10	137	73.64	81.93	85.41			
						CGP55845	sum of two "Equation3"		140	6	1.17	-0.27	1.91	1.01	-0.34	7.46	12.77	134	76.07	90.92	96.66	1.1538	3.30E-01	-8.982
6CE,	50Hz	20s Ctrl	1-10	Norm	+	Control	"Equation3" pooled data	7	150	3	1.12	-2.12	80.00				15.44	147	92.67	100.95	104.72			
S7IO	5Hz	20s CGP				CGP55845	sum of two "Equation3"	8	150	6	1.17	-0.27	1.91	1.15	-4.78	200.25	15.12	144	95.48	110.27	116.55	1.0335	3.80E-01	-9.32
6DE,	50Hz	20s Ctrl	1-10	Norm	+	Control	"Equation3" pooled data	7	130	3	1.01	-0.28	2.45				12.12	127	68.48	76.80	79.95			
S7LO	50Hz	60s Ctrl				CGP55845	sum of two "Equation3"	6	130	6	1.17	-0.27	1.91	0.83	-0.28	2.67	8.60	124	29.81	44.73	49.88	16.9489	**2.75E-09**	**32.07**

Supplementary Table 8. Non linear regressions FIGURE 7 and supplementary figure S8

Stimulation protocol											Model parameters												Model comparison stats		
Figure	Freqency	protocol interval	Protocol repetition	Type of data	eGFP condition	Drug condition	Model	N neurons	N obs	k	A1 control	A2 control	A3 control	A1 DPCPX	A2 DPCPX	A3 DPCPX	SS	df	AIC	AICc	BIC	F	p	dAICc
7A, S8B	5 Hz	20 s	1-10	Raw	-	Control & DPCPX	"Equation3" pooled data	9	198	3	-84.54	14.12	7.73	-84.54	14.12	7.73	347778.43	195	2049.17	2057.38	2062.32			
							sum of two "Equation3"		198	6	-60.78	9.91	4.15	-108.73	19.22	10.73	236918.36	192	1979.17	1993.76	2002.18	29.9472	**6.28E-16**	**63.62**
S8C	5 Hz	20 s	1-10	Norm	-	Control & DPCPX	"Equation3" pooled data	9	180	3	0.97	-0.13	6.15	0.97	-0.13	6.15	7.90	177	-43.96	-35.73	-31.19			
							sum of two "Equation3"		180	6	0.95	-0.09	3.82	0.99	-0.17	7.79	7.85	174	-39.10	-24.45	-16.75	0.3670	7.77E-01	-11.29
7B, S8E	50 Hz	60 s	1-10	Raw	-	Control & DPCPX	"Equation3" pooled data	7	154	3	-84.67	-13.61	0.04	-84.67	-13.61	0.04	786345.89	151	1759.92	1768.18	1772.06			
							sum of two "Equation3"		154	6	-65.61	-28.94	3.47	-119.29	7673.78	3955.37	755965.17	148	1759.85	1774.62	1781.11	1.9826	1.19E-01	-6.43
S8F	50 Hz	60 s	1-10	Norm	-	Control & DPCPX	"Equation3" pooled data	7	140	3	1.20	0.31	3.11	1.20	0.31	3.11	197.12	137	453.20	461.50	464.97			
							sum of two "Equation3"		140	6	1.19	0.56	3.90	1.23	0.06	0.06	194.39	134	457.26	472.10	477.85	0.6257	6.00E-01	-10.6
7C, S8H	50 Hz	20 s	1-10	Raw	-	Control & DPCPX	"Equation3" pooled data	9	198	3	-104.53	-1.83	-3.93	-104.53	-1.83	-3.93	860620.94	195	2228.57	2236.78	2241.73			
							sum of two "Equation3"		198	6	-71.04	-10.90	0.48	-130.34	-18.57	-8.89	798562.47	192	2219.76	2234.34	2242.77	4.9736	**2.40E-03**	**2.44**
S8I	50 Hz	20 s	1-10	Norm	-	Control & DPCPX	"Equation3" pooled data	9	180	3	1.22	-4.07	199.98				64.41	177	333.82	342.05	346.60			
							sum of two "Equation3"		180	6	1.19	0.06	0.69	1.17	-3.72	100.57	61.59	174	331.77	346.42	354.12	2.6551	5.01E-02	-4.366
7D, S8K	5 Hz	20 s	1-10	Raw	+	Control & DPCPX	"Equation3" pooled data	9	198	3	-62.16	17.69	8.91	-62.16	17.69	8.91	238830.83	195	1974.76	1982.97	1987.91			
							sum of two "Equation3"		198	6	-52.92	-17.40	-18.80	-71.29	13.45	4.14	226298.52	192	1970.09	1984.68	1993.10	3.5443	**1.56E-02**	-1.71
S8L	5 Hz	20 s	1-10	Norm	+	Control & DPCPX	"Equation3" pooled data	9	180	3	0.94	-0.27	10.26				14.42	177	64.45	72.68	77.22			
							sum of two "Equation3"		180	6	0.9199	-2.6885	108.479	0.96761	-0.1152	3.43286	14.03	174	65.55	80.20	87.90	1.60	1.91E-01	-7.52
7E, S8N	50 Hz	60 s	1-10	Raw	+	Control & DPCPX	"Equation3" pooled data	7	154	3	-90.97	45.05	2.33	-90.97	45.05	2.33	199289.92	151	1548.53	1556.80	1560.68			
							sum of two "Equation3"		154	6	-77.94	39.98	2.62	-104.10	50.32	2.12	188222.67	148	1545.73	1560.50	1566.99	2.9007	**3.70E-02**	-3.70
S8O	50 Hz	60 s	1-10	Norm	+	Control & DPCPX	"Equation3" pooled data	7	140	3	0.91	-0.30	5.65	0.91	-0.30	5.65	33.82	137	206.44	214.73	218.20			
							sum of two "Equation3"		140	6	0.84	-0.32	2.63	1.10	-0.21	0.06	30.85	134	199.55	214.40	220.14	4.3077	**6.18E-03**	**0.338**
7F	5 Hz	20 s	1-10	Raw	- and +	DPCPX	"Equation3" pooled data	9-	198	3	-89.81	15.26	6.69	-89.81	15.26	6.69	419133.26	195	2086.12	2094.33	2099.27			
							sum of two "Equation3"	9+	198	6	-108.73	19.22	10.73	-71.29	13.45	4.14	343921.71	192	2052.96	2067.55	2075.98	13.9960	**2.73E-08**	**26.78**

Supplementary tables 1-8.
Data analysis, model comparison and statistics.

The tables correspond to the different figures illustrating the comparisons. The column **Figure** indicates the panel of the figure illustrating the conditions compared. In these figures, the averaged eIPSCs amplitudes in the two conditions are illustrated, but statistical analysis were performed using averaged eIPSCs amplitudes of each neurons. These values were calculated by averaging eIPSCs amplitudes of the same rank obtained from reiterations of the protocols. The reiterations used for the average are indicated in the column **Protocol repetition** (usually iterations 1-10). For protocols using trains of stimulations, the **frequency** of stimulations is given (5 Hz or 50 Hz) as well as the time between protocols (20 s or 60 s) in the column **Protocol interval**. The **Type of data** column indicates whether data were averaged raw eIPSCs amplitudes (Raw) or averaged normalized amplitudes (Norm). The **eGFP condition** column indicates whether the data compared were from eGFP- (-) or eGFP+ (+) neurons or both (+ and -). The **Drug condition** column indicates whether the data compared were recorded without (**Control**) or with CGP55845 or DPCPX, or both. The **Model** column indicates the two models compared. **N neurons** corresponds to the number of neurons (eGFP- (-) or eGFP+ (+)). **N obs** corresponds to the number of observations. In experiments with trains of stimulations, the number of observations per neuron and per condition was of 11 for raw data and 10 for normalized data. **k** corresponds to the number of parameters in the model. A1, A2 and A3 are the parameters calculated by non-linear regression (two A1, A2 and A3 are given when a sum of two regressions are used). **SS** is the residual sum of squares calculated with the model. **df** is the degree of freedom of the model. **AIC** is Akaike information criterion; **AICc** is the AIC corrected for small samples; **BIC** is the bayesian information criterion. **F** is the value of the F-distribution of the comparison between the two models. **p** is the corresponding p-value. **dAICc** is the decrease in AICc provided by the model indicated in that line with respect to the model in the line above. A positive value indicate that the model correspond to the most parsimonious explanation with respect to the model in the line above.